Lunds Universitets Naturgeografiska Institution

Seminarieuppsatser Nr. 66

Climate conditions required for re-glaciation of cirques in Rassepautasjtjåkka massif, northern Sweden

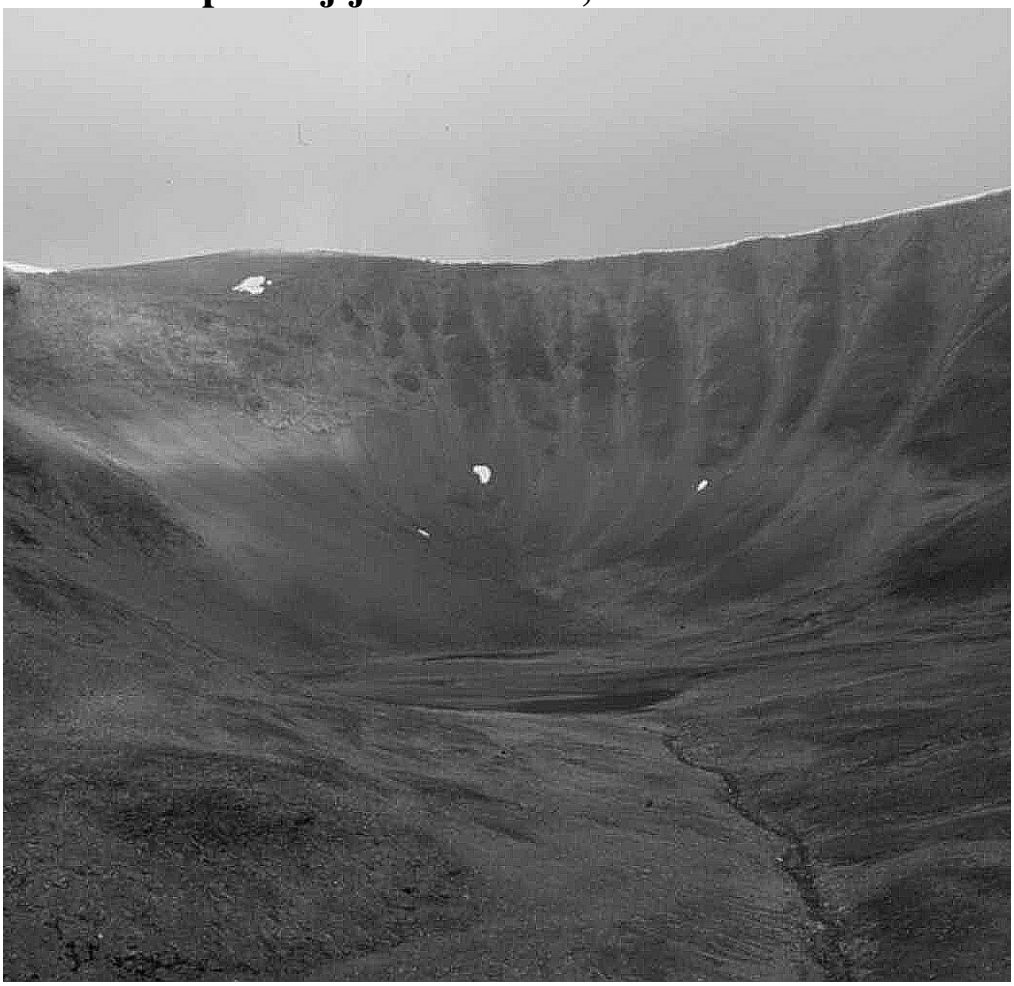

Margareta Johansson

2000

Department of Physical Geography,
Lund University
Sölvegatan 13, S-221 00 Lund,
Sweden

TABLE OF CONTENTS

Abstract

Since the mid 1970s the general retreating trend for glacier in Scandinavian have ceased and some glaciers have even started to advance. This is due to a more maritime influence on the climate, which means increased precipitation in winter and lower summer temperature. A more maritime climate can be said to be favourable for glacier growth. Under such climate conditions is it possible that new glaciers are forming? The aim of this project is to assess the climate conditions that are needed to initiate a glacier in empty cirques in a small mountain massif, the Rassepautasjtjåkka massif, northern Sweden. The study area is of interest since the cirques are located just below the glaciation limit. Since there are no moraines or other signs of glaciation in the area it is still uncertain when the cirques were formed. Using a gridbased temperature index ablation model, that takes into account the topographic effects on melt, the melt during the summer was calculated and the snow that remains at the end of the melt season is what can constitute the ground to a new glacier. Weather data has been collected in the cirques every third hour for the last eight years and this was used as input to the model. The summer mean temperature needs to be lowered between –2 °C and –3 °C from the current climate before snow will remain after a melt season. An increased initial snow cover of today between 100-150% (under otherwise equal conditions) will have the same effect i. e remaining snow at the end of the melt season. When increasing the initial snow cover with 50% and lower the summer mean temperature by –2 °C, snow will be left in the cirques after a melt season. The climate conditions that are required to create a re-glaciation are not met by conditions evaluated from proxy-data from the Holocene. Therefore it can be concluded that glacier has not existed in the Rassepautasjtjåkka massif during the Holocene and that the origin of the cirques extends further back than the Holocene. According to future climate scenarios that predict increased temperature and increased precipitation glaciers will not form in the cirques in the future spanned by the predictions.

Acknowledgement

Thanks to the Göran Gustafsson Foundation who supported the fieldwork in August 1999. I would also like to thank my supervisor at the Department of Physical Geography, Lund, associate professor Lars Bärring for all support and good ideas. Further I would like to thank Dr. Regine Hock (Climate Impact Research Centre, Kiruna) for an interesting project, for supporting and encouraging me and also for a nice hiking in the mountain with a non-functional mobile phone, or? I am also very thankful to associate professor Peter Jansson (Department of Physical Geography, Stockholm) that has improved my thesis, supported and encouraged me. Jonathan, I can't dedicate a whole page to you even though you were Regines and my Sherpa for three days, but thanks anyhow. I would also like to thank all the people who has been involved in this project during the years and has contributed to the data used in this project. Finally I would like to thank Martin for encouraging me when I was in great need of it.

1 Introduction

1.1 Background

During the last century, glaciers have retreated worldwide. In northern Sweden this trend started at the beginning of the 20th century after many glaciers had reached their maximum extension in response to a climatic deterioration often referred to as the "Little Ice Age" (Grove, 1988). Examples of glaciers that reached their maximum extension are Storglaciären 1910, Mikkaglaciären 1915 (Holmlund, 1987), Sydöstra Kaskasatjåkkoglaciären and Tarfalaglaciären (Grudd, 1990). For most of the 20th century mass balance (the sum of one winters accumulation and the following summers ablation) has been negative i. e. the front has retreated and a mass loss has occurred due to a 1°C increase in summer mean temperature. In the 1970s the negative trend ceased (Holmlund, 1987).

There is a general coupling between atmospheric circulation and the glacier mass balance (Hoinkes, 1968; Alt, 1987; Pohjola and Rogers, 1997). Glaciers in areas with frequent occurrence of high pressure, referred to as continental climate, owe their existence to low temperatures. Fluctuations in mass balance are strongly correlated to mean summer temperature. In contrast, glaciers situated in areas with high frequency of cyclonic storms, referred to as maritime climate, form in response to high winter snowfall. Cyclonic storms that occur in winter increase the winter accumulation. On the contrary, a high frequency of anticyclonic patterns reduces accumulation in the winter and increases snowmelt in the summer (Hooke, 1998).

Much of the variability in surface temperature and precipitation patterns during the winter over Europe can be explained by the North Atlantic Oscillation (NAO) (Hurrell, 1995). The NAO index is traditional defined as the difference in pressure between Iceland and the Azores. Since the early 1970s a positive trend, i. e. a large difference in pressure, is indicated by the index, with the highest values in late 1980s and early 1990s (Jones *et al*., 1997). The large difference in pressure induces the westerlies and contributes to a more maritime climate. A more maritime climate will decrease the yearly temperature amplitude, the warmer winters will generate more precipitation and the colder summer will decrease the melt rate. By using the Tarfala temperature record Grudd and Schneider (1996) have detected decreasing yearly amplitude between the coldest winter months and the warmest month of the following summer by 0.8 °C per decade between 1965-1995. This indicates a change towards a more maritime climate in the northern part of Sweden. Mass balance studies and glacier front observation from these areas have shown that many glaciers in Scandinavia and Iceland have shown a positive mass balance and the glaciers have started to expand (Holmlund *et al*, 1996). The current climate in Scandinavia can be said to be favourable for glacier growth. The question may then be asked; is it possible for new glaciers to form?

In order to assess the likelihood of initiating a glacier, Jonsson and Jansson (1993) installed a weather station, in an empty cirque in the Rassepautasjtjåkka massif, northern Sweden. Questions have been raised concerning when and how, many of the empty cirques in northern Sweden have been formed (Holmlund, 1990). Many of these cirques lack signs of glaciations during the Holocene. Their origin are not known, but they are assumed to originate from mountain glaciations either at the beginning or at the end of an ice age, or both. By studying the local climate in an empty cirque its origin might be revealed (Jonsson and Jansson, 1993).

Jansson *et al* (1999) made a qualitative assessment of the requirements for cirque formation based on among other thing the geomorphology and the current climate conditions in the study area. They concluded that either a significant change in precipitation and wind regime or a moderate change in temperature was required to initiate a glacier in the Rassepautasjtjåkka massif. The melt conditions were found to be quite regionally uniform but the precipitation was governed by regional gradients and local conditions and they assumed that the snow accumulation decreased towards the east. Further the authors concluded that a lowering of the temperature would only lead to a cold-based non-erosive glacier and in order to form a wet-based erosive glacier, warmer winters with higher accumulation rates were required, i. e. a more maritime influence. Favourable conditions for increased precipitation would be a strong zonal circulation associated with a northerly position of the polar front. They also concluded that the cirques could not have been formed by an ice sheet flow since the cirques face in all directions. Using typical erosion rates (1 mm a^{-1}) at least 0.3 million years may be required to form a cirque in the massif. Lack of moraines and other sign of recent glaciation in the cirques indicate that there have not existed any glaciers during Holocene (Jansson *et al*., 1999).

1.2 Aim of the study

This study is a continuation of a project started in 1992 by Jonsson and Jansson (1993), and the aim is to quantitatively assess the conditions that are required to achieve re-glaciation in the cirques in the Rassepautasjtjåkka massif, northern Sweden. This is a sensitivity study that partly investigates the sensitivity of a melt model and also the sensitivity of the melt rate when changing climate parameters. The Rassepautasjtjåkka massif is of interest since this site is located only 25 kilometres from the Kebnekaise massif, where many glaciers have been experiencing growth during the last decades. Only five kilometres west of Rassepautasjtjåkka two glaciers (Mårmaglaciären and Mårmapakteglaciären) are located on almost the same altitude as the empty cirques. How come there are no glaciers in the empty cirques and what would it take in terms of climate change to initiate a re-glaciation?

The snow cover that remains after a melt season is what can constitute the basis for glacier initiation and growth. A major source of energy for melt is global radiation (Ohmura *et al*., 1992) and it is therefore relevant to see how the amount of energy varies both spatially and temporally. By using a grid-based high-resolution ablation model, the total amount of melt during a season can be simulated and the effect of a climate change is quantitatively assessed.

The specific objectives are:

- To estimate topographic effects on spatial distribution of potential clear-sky direct solar radiation and snow melt in the empty cirques
- To assess the climate conditions that are needed to initiate glaciation in the cirques by changing either the initial snow cover, the temperature or both.

2 Area description

Rassepautasjtjåkka (68°05´ N, 18°50´ E) is a small mountain massif located in the northern-most part of Sweden, approximately 25 km NE of the Kebnekaise massif and the Tarfala research station (Figure 1). The area is roughly 40 km^2 and the elevation in the area ranges from 1080 to 1728 m a.s.l. The glaciation limit in the area is inferred to be at 1820 m a. s. l. (Østrem, 1964). In this area there are four well-developed cirques and some less developed ones. The distinct cirques are approximately 1 km wide and located just below the glaciation limit. Two cirques are facing towards the southeast and one towards the northeast and the fourth is facing towards the southwest. The automatic weather station that was installed in the beginning of the 1990s is placed in the cirque facing towards the southwest; referred to as the central cirque (Figure 2).

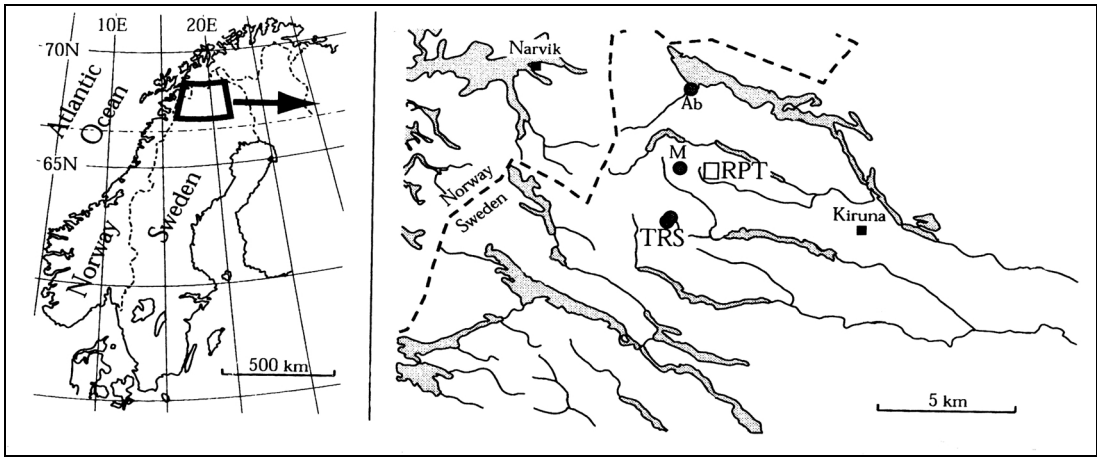

Figure 1. The location of the Rassepautasjtjåkka massif and it surroundings; Rassepautasjtjåkka, the study area (RPT), Tarfala Research Station (TRS), the Mårmaglaciären (M), and Abisko (Ab) (Jansson et al., 1999).

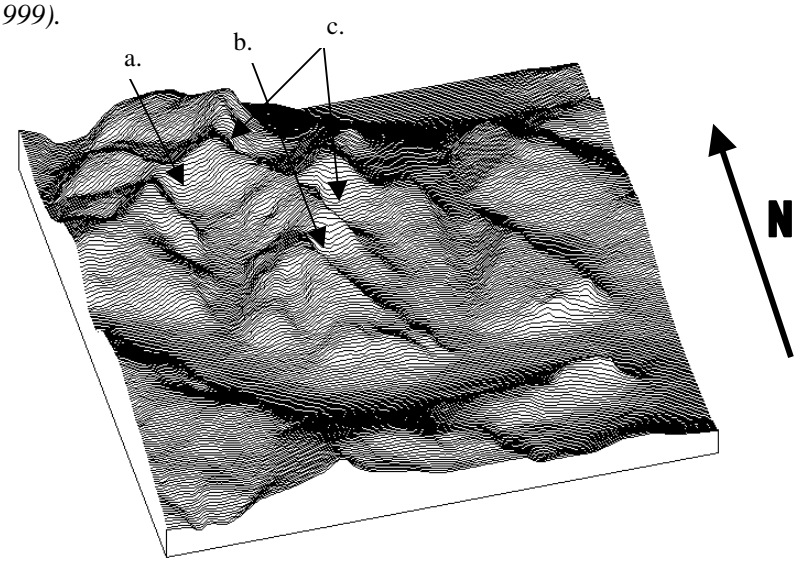

Figure 2. The Rassepautasjtjåkka massif with the central cirque (a) where the climate station is located, the eastern cirque (b), and the two other well-developed cirques (c).

Perennial snow patches are found on the top of the mountain ridge separating the four cirques. There are perennial snowfields on the northeast-facing slopes in all but the central cirque. The central cirque is facing towards the southwest and the perennial snowfield is instead found on the slopes facing the east and the west. To the southwest of the site, the area is characterised by steep walled, glaciated mountain massif like Kebnekaise, whilst to the north the peaks are more rounded and separated by large U-shaped valleys.

From field observation the geomorphology of the area can be said to be characterised by frost action. Pattern ground is widespread and block fields are a common feature. The annual mean temperature at the climate station for the period 1993-1998 is -4.7 °C (Table 1 and Figure 3). The summer mean temperature (June to August) is 4.1 °C and the winter (September to May) is -7.6 °C. Annual and winter mean temperature is not calculated for 1997 since there is one month missing data and in 1999 the data has so far just been available until the 27 August.

Table 1. Annual (January – December), summer (June – August) and winter (September the preceding year – May) mean temperature for the period 1993-1999.

	1993	1994	1995	1996	1997	1998	1999	Mean whole period
Annual temp °C.	-4.2	-4.4	-4.9	-4.5	-	-5.4	-	-4.7
Summer temp °C	3. 6	4.3	3.5	4.7	6.4	3.5	2.7*	4.1
Winter temp °C	92-93 –6.8	93-94 –7.7	94-95 –7.3	95-96 –7.5	96-97 -	97-98 –8.0	98-99 –8.2	-7.6

* Four days missing values in the end of August.

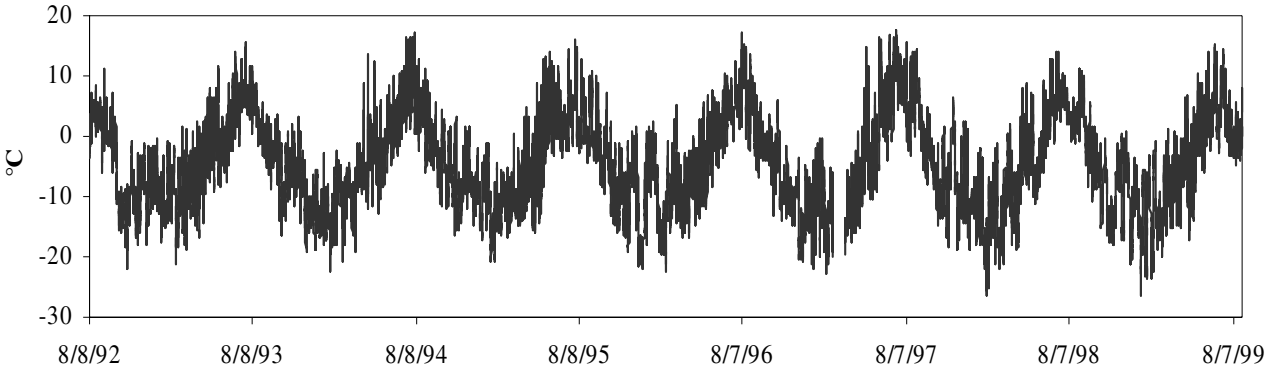

Figure 3. Air temperature (momentary value each three hours) recorded at the climate station for the years 1992 to 1999

3 Theory

3.1 Definition of a glacier

Many definitions of a glacier can be found in the literature. In simple terms the glacier can be said to be a body consisting mainly of recrystallized snow, that shows evidence of down-slope or outward movement due to the pull of gravity (Skinner and Porter, 1987). A more thorough definition of a glacier from Jonsson (1981) says that a glacier is an object that fulfils three criteria:

- It is a mass of snow/ice that is well defined from the surrounding area.
- A dominating part of the ice configuration must have been made from snow by the pressure of the glacier.
- The ice needs to move in at least one particular direction.

The third criterion makes it easy to distinguish a perennial snowfield from a glacier. There can be ice in the lower part of a perennial snow patch as well, but the total thickness of the snow patch is too small to create the pressure necessary for deforming, i. e. moving, the ice. The extent of ice movement can vary considerable. The speed will increase with increasing thickness and with an increasing slope angle. Ice temperature is another important factor, the warmer the ice is the easier it deforms. Since many factors control the internal deformation, it is hard to determine a certain thickness that distinguishes a perennial snowfield from a glacier. It is commonly said that the thickness of ice needed for internal deformation is about 30 m (Jonsson, 1981). The mean ice depth of a glacier can vary greatly. The Tarfala glacier, with a mean ice depth of 19 meter, is one example of a thin glacier (Grudd, 1990).

3.2 Melt condition

When the snow/ice temperature is at or near 0 °C the snow/ice will start to melt, the quantity being determined by the amount of energy available. The amount of energy available for melt is determined from the energy budget (Male and Gray, 1981). The energy budget of snow/ice is complex e.g because of the penetration of short-wave radiation into the snow pack and also because of the internal water movement (transport of sensible heat) and phase changes (latent heat) (Oke, 1987). The energy budget for a volume of snow/ice whose upper surface is in contact with the air and its lower is in contact with the ground can be written as

$$Q_m = Q_{sn} + Q_{ln} + Q_h + Q_e + Q_g + Q_p - dU/dt \qquad (1)$$

where Q_m is the energy flux available for melt, Q_{sn} is the net short-wave radiation flux absorbed by the snow and Q_{ln} is the net long wave radiation flux at the snow-air interface. Q_h is the sensible heat flux from the air at the snow/ice-air interface, Q_e is the net convective latent heat flux (evaporation, sublimation, condensation) at the snow/ice-ground interface and Q_g is the conductive heat flux of the snow/ice-ground interface. Q_p is the sensible heat flux from rain and dU/dt is the rate of change of internal energy per unit area of snow/ice cover (Male and Gray, 1981). Fluxes that only take place at the snow/ice-air interface are the net long-wave radiation and the convective heat transfer processes. The short-wave radiation exchange occurs mainly at the surface although limited amounts of short-wave radiation penetrate into the snow/ice pack.

The ground heat flux, that is usually small, may produce small amounts of melt near the ground. The only time that water is released from this lower layer is when the snow/ice is holding maximum liquid and the snow/ice reaches 0 °C. Rain can penetrate deep down in the snow/ice and represent an additional heat source for the pack. This added heat is distributed more uniformly through out the pack than the heat obtained from other sources (Male and Gray, 1981). Models that are based on this type of energy equation that account for internal redistribution of energy require a large number of inputs variables and these data are not available for the study area. Therefore an energy balance model could not be applied and a temperature index model that requires less input data was applied instead.

3.3 Model description

To calculate the progressive melt and the recession of the snow line during a summer a distributed temperature index melt model was used in this study (Hock, 1998). In general, a temperature index model, also referred to as a degree-day model is based on an assumed relationship between ablation and temperature. The factor of proportionality is the degree-day factor (DDF), defined by the melt divided by temperature. Temperature index models are the most commonly used method of melt computations due to their simplicity (Hock, 1998). A classical degree-day model can be defined as

$$M = \begin{cases} \frac{1}{n} DDF_{snow/ice} & T :> 0 \\ 0 & T : \leq 0 \end{cases} \qquad (2)$$

where M is the melt rate (mm h^{-1}), n is the number of time steps per day (if the time step is 1 hour n=24), T is the temperature and $DDF_{snow/ice}$ is the degree-day factor (mm d^{-1} °C^{-1}) different for snow and ice. The degree-day factor for ice is due to lower albedo, expected to exceed that for snow. Since the $DDF_{snow/ice}$ are assumed to be constant in time and space, the computed melt rate over snow and ice is only a function of air temperature (Hock, 1999).

According to Hock (1998) the classical degree-day models have two major disadvantages. The first is the low temporal resolution. The result from a simple degree-day model will be acceptable if the temporal resolution are sparse, but if the temporal resolution will increase then the accuracy of the result will not increase. The second drawback is that the ordinary models do not include a spatially differentiated melt rate. Usually, the degree-day factor is assumed to be constant over an area, but melt rates can vary much in space due to the influence of the topography on the radiation conditions. This is especially pronounced in high mountainous regions (Hock, 1998). Topographic shading, aspect and slope angles have a strong influence on the spatial distribution of global radiation, and thus on melt. Global radiation is generally regarded as a major source of energy for melt (Ohmura *et al*., 1992). The spatial distribution of melt rate that results from a classical degree-day model will be uniform since it neglects topographic effects like slope, aspect and usually only includes the effect of elevation via the temperature lapse rate. A classical degree-day model can represent the mean melt rates but not the large spatial and temporal variations in melt.

The model used in this project is a modified temperature index model (Hock, 1998) that takes into account the spatial and temporal distribution of melt. It is easy to apply in many different areas since air temperature and a digital elevation model are the only input needed. A radiation

index is determined by the model in terms of potential direct solar radiation at the surface and it is derived from the following considerations:

- Potential solar radiation is subject to pronounced daily cycles, similar to those generally observed for melt rates.
- It introduces a distinct spatial element, because it considers topographic effects as slope angle, aspect and effective horizon.
- The computation of the radiation index does not require any meteorological data, but can easily be approximated by well-known algorithms on insolation geometry and topography.

Potential clear-sky direct solar radiation is used instead of global radiation (diffuse and direct solar radiation), in order to avoid additional meteorological data such as cloud observations. Slope and aspect is calculated for each grid cell in a digital elevation model. The digital elevation model must cover a larger area than that area where melt is to be calculated, since the surrounding area can shade the area of interest. Topographic shading is computed based on the effective horizon and the position of the sun. The equation used to calculate the potential clear-sky direct solar radiation *(I)* is expressed as:

$$I = I_0 \left(\frac{R_m}{R} \right)^2 \quad \psi_a \left(\frac{p}{p_0 \cdot \cos Z} \right) \quad \cos \theta \tag{3}$$

where I_0 is the solar constant (1368 W/m^2) and $(R_m/R)^2$ is the eccentricity correction factor of the Earth orbit for the time considered with R the immediate and R_m the mean distance between the sun and Earth. ψ_a is the mean atmospheric clear-sky transmissivity, p the atmospheric pressure and p_0 the mean atmospheric pressure at sea level. Z is the local zenith angle (the angle between the solar beams and the normal to the ground surface) and $\cos\theta$ is the angle of incidence based on the slope angle, zenith angle, solar azimuth and slope azimuth angle. I is calculated as a function of the top of atmosphere solar radiation, an assumed atmospheric transmissivity, solar geometry and topographic characteristics. The clear-sky transmissivity is assumed to have a constant value of 0.75. Other studies (Oke, 1987) have reported the value within the range of 0.6 and 0.9. The ratio between p / p_0 includes the effect of altitude and results in higher direct radiation at higher elevations (Hock, 1998). The calculated potential solar radiation is incorporated in the temperature index model that calculates the ablation *(M)*:

$$M = \begin{cases} \left(\frac{1}{n} MF + a_{snow/ice} \cdot I \right) \cdot T & : > 0 \\ 0 & T : \leq 0 \end{cases} \tag{4}$$

where MF is the melt factor (mm d^{-1} °C^{-1}), $a_{snow/ice}$ is the radiation coefficient different for snow and ice and I is the potential clear-sky direct solar radiation at the ice or snow surface (W/m^2). T is the air temperature (°C) n is the number of time steps per day. The melt factor and the radiation factors for snow and ice are empirical coefficients. The radiation coefficent for ice is due to lower albedo, expected to exceed that for snow. The melt factor used in Equation 4 cannot be compared to ordinary *DDF* (Equation 2), since the *MF* is no longer a linear relationship between temperature and melt, but it also include the potential direct solar radiation for snow and a radiation factor for snow/ice.

4 Method

4.1 Field measurements and fieldwork

In August 1992 a weather station was installed at approximately 1260 m a.s.l. in the central cirque in the Rassepautasjtjåkka massif (Appendix A). Air temperature, global radiation, wind speed, wind direction, air pressure and humidity have been measured every third hour since 1992, except for the break in February 1997 (Figure 3 and Appendix B). The air temperature data were used as input for the melt calculations. The accumulated snow cover has been measured for three years (1993, 1995 and 1999). The snow depth surveys were carried out in two well-developed cirques. The original plan was to measure the snow cover in all four distinct cirques in the massif, but due to a snowstorm, only two were investigated in 1993 (Jansson *et al*, 1994). The climate station has been visited once or twice every year since it was installed, except for 1997. In 1995 snow density pits were dug in both the investigated cirques (Jansson and Jonsson, 1996).

During the 25th and the 27th of August 1999, fieldwork was carried out in the Rassepautasjtjåkka massif. The aim was to map the current snow lines both in the massif and in the surrounding areas. This was later going to be used as a key to the model when it was run and calibrated. Another reason was to exchange the data-storing unit on the weather station in order to collect the climate data of the summer. The geomorphology in the area was also interpreted to find any signs of earlier glaciations. No moraines, glacial melt channel or any other signs were found.

4.2 Input data to the model

The model requires climate data, a digital elevation model (DEM) and derived digital terrain information as input data (Table 2).

Table 2. Input data required by the model.

Input data	Description
Climate data	Recorded temperature data.
DEM 1	A digital elevation model that covers an area larger than the area to be calculated.
DEM 2	Elevation data for the area to be calculated i. e. the cirques.
DEM 3	Elevation data for the area that is glaciated.
DTM 1	Calculated slope for the same area as the DEM1.
DTM 2	Calculated aspect for the same area as the DEM1.
DTM 3	Delimits the firn area on a glacier, where firn is set to be 1 and the rest is set to be zero.
DTM 4	The initial snow cover in water equivalent, covering the same area as DEM 2.

4.2.1 Input climate data and evaluation of the climate data with data from Tarfala

Climate data collected every third hour from the weather station in the central cirque is used as input to the model. The input file must contain Julian day, time, and the climate data in different columns. The model requires input data from midnight (Swedish standard time) and onwards in equidistant time steps. If the model is run with a three hourly time step there must be data available at 00.00, 03.00, 06.00 etc., every day that is to be calculated.

The measurements have not been carried out at the same hours every year, since the logger cannot start at a preset time, but starts in the required interval when the storage module is exchanged. For example in 1998 the weather station was started at 8.15 (Swedish standard time) and the measurements have been done at 11.15, 14.15 etc. Since the study area is hard to access the data-storing unit is exchanged when opportunities have been given (Table 3). To meet the requirements demanded by the model some generalisation has been made, the value closest to the correct time step has been used. For example, for 1998 the time used for the model was 9.00 instead of 8.15, which was the time when the weather data was actually recorded. A few missing weather data (approximately 0.01‰) were filled in using linear interpolation.

Table 3. Starting time and the time used in the model for the different periods.

Period	Starting time (Summer time)	Swedish standard time	Time used in model
920805-930502	15.05	14.05	15.00
930502-930826	16.20	15.20	15.00
930826-940730	15.17	14.17	15.00
940730-950901	14.03	13.03	12.00
950901-960914	14.19	13.19	12.00
960914-980406	12.00	11.00	12.00
980406-990423	09.15	08.15	09.00
990423-990827	14.00	13.00	12.00

To detect any potential inconsistencies in the data the Rassepautasjtjåkka temperature record was compared to the Tarfala temperature record (Figure 4). This was done for all three years with measured initial snow cover. Both temperature records show the same trend. Temperature rise and fall occurs at the same time, but not to the same extension.

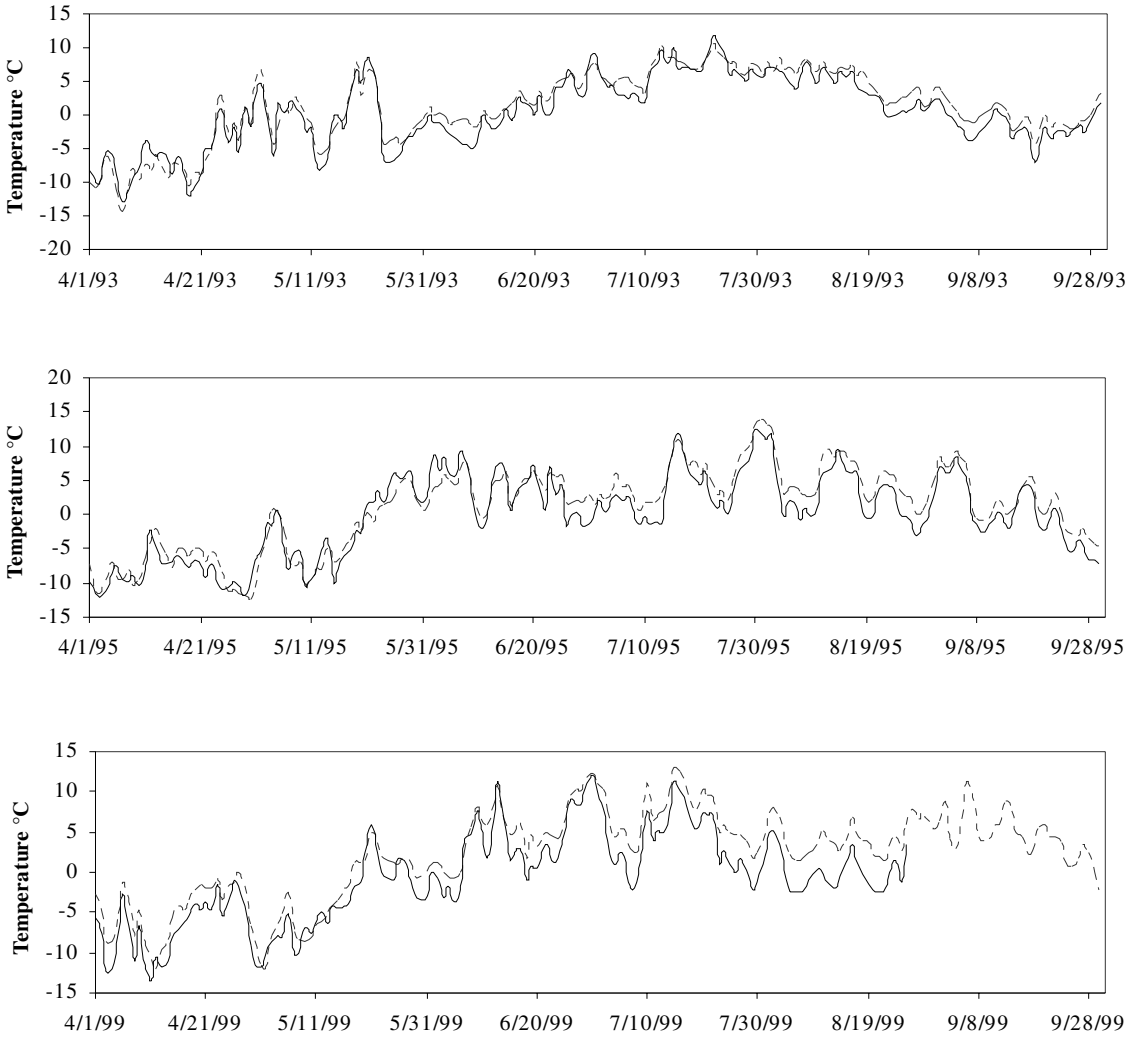

Figure 4. Comparison between the temperature in Rassepautasjtjåkka (full line) and Tarfala (dotted line) during the period April to September 1993 (top), 1995 (middle) and 1999 (bottom).

4.2.2 DEM and DTM

A digital elevation model (DEM 1) is needed as input to the ablation model and it must cover a larger area than the area where ablation is to be calculated. A DEM was constructed from the Fjällkartan, sheet BD6, scale 1:100 000. The contour lines were digitised from an enlarged copy of the map (1:50 000) using the program Cartalinx. Every 40 m contour line was digitised. The RMS-error, the measure of the variability of measurements about their true values (Hagan *et al*, 1998), was approximately 11 m. The arcs were rasterised using the software IDRISI (Eastman, 1997). The rasterised arcs were then interpolated to represent the whole area.

The interpolation method used is INTERCON that uses a modification of the CONSURF algorithm (Eastman, 1997). First, profiles are constructed around the four edges of the map to produce a completely closed spaced i. e. all regions of unknown height are bounded by known heights. The four corner points and any contours, which intersect the edges, are used to construct the bounding profiles. Then a set of horizontal profiles across each row is created using the edge profiles and any contours crossed by the horizontal scan. At each cell of unknown height, the interpolated profile height is recorded along with the slope of the profile at that point. Profiles are then constructed in subsequent passes vertically along the columns and diagonally from left to right and right to left across the image. The final height recorded for each cell is that of the profile with the maximum slope. The likelihood to find an error exceeding half a contour line is almost equal to 1 % (Eastman, 1997). A lowpass filter was used after the interpolation to remove some of the angularity of the linear interpolation. The height in the four corners was determined from the map. The final DEM covers the region 1624 to 1636 and 7550 to 7562 in the Swedish national reference system RT38 2.5gon V and the resolution is 50 m.

A common problem when using contour lines as input to a DEM is the formation of terraces on slopes. This is a consequence of the unevenly distributed point data characterised by a larger number of points along the contour line but very few in between the lines. Clustering of the contours is a common problem as well. Eklundh and Mårtensson (1995) concluded that this was a problem especially pronounced when using Intercon. In areas with short distance between the contour lines this is however, less of a problem. This is the case in the study area; therefore the clustering problem is reduced.

Two additional DEM are required by Hock´s (1998) model. The first delimits the area where melt is to be calculated i. e. the cirques (DEM 2), and the second delimits the glaciated area (DEM 3). The DEM delimiting the glaciated areas is needed to decide whether or not melt continues after the initial snow cover has melted away, which is the case if the calculations is done on a glacier. In this study the DEM3 contained missing values since there aren't any glacier in the area. Both the additional DEM were made by demarcating the cirques using IDRISI.

Digital terrain models (DTM) are needed as an input to the temperature index model. Two in order to calculate the potential clear-sky direct solar radiation in the area. The DTM (DTM 1) that contains slope is calculated as the maximum change in elevation for each cell to its neighbours (3 x 3 window). A new grid is created where each grid cell represents a continuous slope value in degrees. Aspect is derived in ArcView were the steepest down–slope direction is identified from each cell to its neighbours. The values of the output grid represent the compass direction of the aspect; 0 is true north, a 90-degree aspect is to the east, and so forth (DTM 2). One DTM (DTM 3) distinguishes the firn area. Missing values were used since there is a lack of real firn areas in the study area.

A DTM containing the initial snow cover at the starting date of the modelling are required for each period to be calculated (DTM 4). Snow depth measurements have been carried out for three years, 1993, 1995 and 1999 in a radial pattern. The snow depth must be available for the same area that is to be calculated (DEM2). The snow density was measured for both the eastern and the central cirque in 1995, and the average snow density for both cirques was 0.35 kg/m^3. Since there is a lack of density measurements from all the years with initial snow cover, the density is assumed to be the same for all three years. This assumption is justified in this sensitivity study since the initial snow cover measurements are made at approximately the same time of the year.

There are only snow measurements from two out of the four cirques and therefore an assumption is made that the circumstances was similar in the other two cirques. The upper eastern cirque is assumed to have the same snow conditions as the eastern cirque and the northeast-facing cirque is assumed to have similar snow cover as the central cirque. The position of the measured initial snow cover points was not known. The approximate co-ordinates for the measured points were therefore determined from a map.

The number of snow depths measurements used as input to the DTM containing initial snow cover were few ranging from 20 to 40 in each cirque. Semiovariograms were calculated but it was not possible to fit any specific model. This is probably due to the few input data points. The measured point data was however interpolated in Surfer using kriging interpolation and the default variogram model, that is a linear model. Kriging is an advanced elaboration of the inverse distance weighted moving average. The method involves taking the weighted sum of the points within a zone of influence. Kriging considers three important factors in surface modelling. These are distance, clustering and spatial autocorrelation (Bonham-Carter, 1997). The measured cirques were interpolated individually in order to not affect each other. The different interpolations were then pasted together in IDRISI to yield the files containing initial snow cover (m w. eq.) for the four cirques.

On extremely steep slopes the snow will not be able to accumulate. Due to the influence of wind and gravity the snow cover tends to decrease with increasing slope angle. An attempt to include this effect in the interpolated water equivalent files has been made. The angle of repose for cohesion lies between 30° and 40° the snow is expected to be unstable on steeper inclines. Avalanches start most frequently on slopes with average inclination between 30° and 45° but generally not on slopes with inclination >60°, since small sluffs occur during snowfalls unloading the slopes continuously (Schaerer, 1981).

Golding (1974) found a 6 to 8% decrease in water equivalent per 10% slope increase in Alberta, Canada. For the Swiss Alps Witmer (1984) reported a linear decrease of snow depths between 35 and 50° and above that limit the snow depth was set to be zero. In Lägental in Tirol this limit was 60° (Blösch and Kirnbauer, 1992). Whether or not the snow will be able to stay on a slope also depends on whether the climate is continental or maritime. In areas with maritime climate snow is deposited when the temperature is around 0°C and therefore it metamorphoses quickly. This allows the snow to rapidly form a strong bond to the ground also at steep slopes. If the climate is continental the snow will fall at lower temperatures. Since the snow is dry it has more difficult to form bonds, this because the metamorphosis are very slow. For Lägental the climate is said to be something in between maritime and continental and the snow cover in Lägental is assumed to be constant between 0 and 10° and to decrease linearly between 10 and 60°. Slope angles larger than 60°C was assumed to be free from snow (Blösch *et al*, 1991). The same assumption is used for Rassepautasjtjåkka. The study area did not contain any slope angle that exceeded 60° since the resolution of the interpolated snow cover files was 50 m and because of this no pixels in DTM4 was set to be free from snow.

Based on measurements, Jansson (personal communication, 1999) concluded that the assumption of a linearly decreasing snow cover between 10-60° was correct if the new value did not deviate from the measured point value more than 0.5 m. This could be said to be the approximately error in the initial snow cover measurements. This is because the surface is covered with weathered blocks and the snow depth will vary if the measurements have been done next to or on a block. Evaluation of the result showed that the originally measurements were only affected marginally

when applying a linearly declining snow cover (Appendix C). There was one measured point that was exceeding the approximate error, but since this was the only point this did not change the approach of using a decreasing snow depth with increasing slope angle. Figure 5 shows the initial snow cover covering the four cirques for the different years.

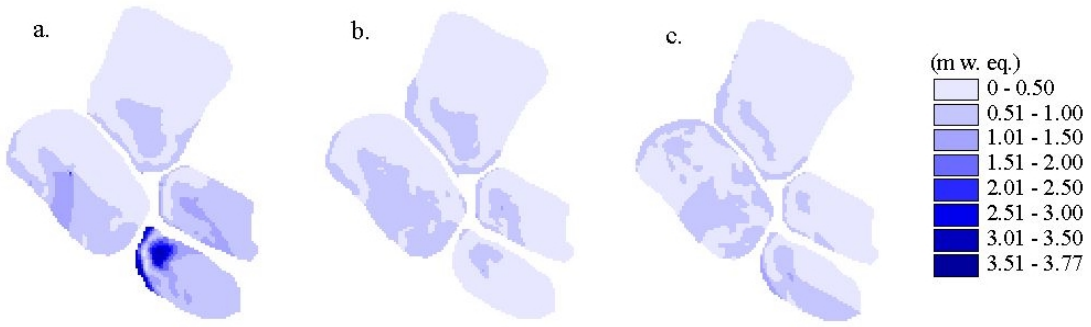

Figure 5. Interpolated snow cover in the end of April in 1993 (a), in 1995 (b) and in 1999 (c).

Many generalisations had to be made when constructing the initial snow cover files. The first is to assume that the snow conditions were similar for the cirques. Another source of error is the co-ordinates for the measured points that were derived from the map. This can have an effect on the actual position of the measured snow depth in all directions. The snow densities were assumed to be the same for all three years, which may not be the case. Since this is a sensitivity study, these generalisations and assumptions are acceptable.

To be able to assess the importance of topography of the surrounding area on potential solar radiation and melt distribution, a DEM1 with a flat area was made. The mean elevation for the area covered by the DEM was calculated and the altitude used in this DEM was 1189 m. Slope and aspect were set to be zero when running the model.

4.3 Calibration of the model

The temperature index model needs to be calibrated for every new area in which it is applied since the factors that influence the melt may vary from one site to another. Three parameters can be changed in order to calibrate the model (Equation 4), the melt factor *MF*, the radiation factor for snow a_{snow} and the radiation factor for ice a_{ice}. Only the two first parameters are of relevance in this study, as there are no glaciers in the area.

a_{snow} affects the spatial distribution of melt because it is multiplied by the calculated potential clear-sky direct solar radiation (Equation 4). Increases in *MF* results in a rather homogenous increase in melt over the study area. In order to demonstrate the sensitivity of the model, a_{snow} was held constant $0.6 * 10^3$ and by varying the *MF*, its influence on melt could be analysed. The opposite scenario with a constant *MF* (1.8 mm d^{-1} $°C^{-1}$) showed the influence of a_{snow} on the melt. Figure 6 shows how the melt is affected by the different parameters. A linear relationship can be found in both graphs and this is due to the construction of the model (Equation 4). The data input used is unlimited source of snow and equal climate conditions. The snowmelt presented in figure 6 represent the mean accumulated melt during a melt season (May- August).

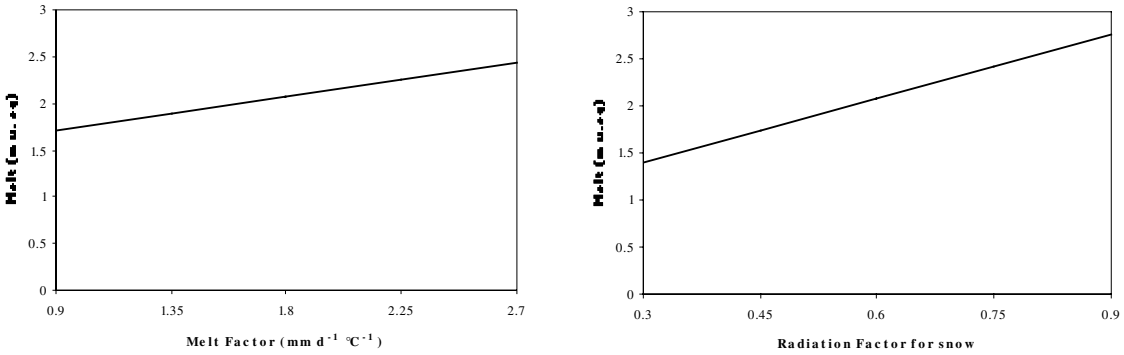

Figure 6. The effect of MF and a_{snow} *on snow melt in the study area. The melt presented is the accumulated mean melt during a melt season.*

The model has been tested and calibrated on Storglaciären by Hock (1998). In that case the modelled ablation was compared to the measured ablation derived from ablation stakes (stakes placed on the glacier) and simulated glacial runoff compared to measured runoff. The model has never been used at a site without a glacier before. The fact that a glacier is absent and hence that snow measurements during a melt season is not carried out is a disadvantage when calibrating the model, since there is no independent validation data available. In this sensitivity study the approach to this problem is to make assumptions based on a comparison between the Tarfala valley and Rassepautasjtjåkka and also between Mårmaglaciären and Rassepautasjtjåkka (Figure 1). Tarfala has a well-documented snow cover and can be used to get a picture of the general melt pattern in the area. Comparison of the actual amount of accumulation and ablation between Tarfala and Rassepautasjtjåkka has on the other hand not been done because there is little agreement between the two. For example, the accumulation on Storglaciären, Tarfala in 1995 was large whereas the measured snow depth in Rassepautasjtjåkka was low in the cirques (Jansson and Jonsson, 1996). The mass balance of the Mårmaglaciären is chosen since this glacier is located very close to the study area and it could help to reveal the local snow conditions during the years.

The years with measured initial snow cover will be used as an input to the model for the calibration. The largest amount of snow was measured in the cirques in 1993. Jansson *et al.* (1994) describe the initial snow cover in this year as very unevenly distributed over the site. The accumulation in the central cirque was small, 1-2 m but in the eastern cirque the snow depth varied between 4 and 10 m. There are large discrepancies between the measured initial snow cover for the different years (Figure 5). In 1995 the measured initial snow cover was relatively thin and in 1999 the measured snow cover was something in between.

The snow tends to melt away at the beginning of July in the Tarfala valley. By using slides the snow cover extent in the Tarfala valley was determined to be approximately 75% at the end of June 1993 and 1999. In 1993 the accumulation on the Mårmaglaciären was unusually high when compared to the other years in the 1990s, it was 1.40 m w. eq. The mass balance this year was +0.27 m w. eq (Bodin, 1994). In 1995 the net balance on the Mårmaglaciären was according to Karlöf *et al*. (1996) +0.1 m w. eq. (winter balance 1.11 m w. eq. and summer balance -0.98 m w. eq.). There are no measurements available yet for 1999 (Table 4).

Table 4. Data used to make a qualitative assessment of the approximate time when the snow cover disappears in the Rassepautasjtjåkka massif.

	Rassepautasjtjåkka snow conditions	Mårmaglaciären mass balance	Tarfala valley snow cover
1993	Large amount of snow measured in the cirques.	Unusually large positive mass balance + 0.27 m w. eq.	At the end of July, 25% of the snow cover in the valley has melted away.
1995	Small accumulation.	Positive mass balance +0.1 m w. eq.	--
1999	Larger accumulation than 1995, but less than 1993.	No measurements available	Similar conditions in the valley as 1993.

The summer temperature is quite uniform when comparing 1993 and 1995. In 1999 the summer temperature was lower than the average for the 1990s (Table 1). Based on this analyses following assumptions are made for this calibration:

- Years with a greater amount of initial snow will become free from snow later in the season compared to those with less snow, under the assumption of otherwise equal summer temperature conditions.
- The initial snow cover that melts at the end of the melt season should be located at and around the perennial snowfields in the area (that were mapped in the end of August, 1999).
- The snow will disappear around mid July, as is the case in Tarfala.
- During years with high accumulation on Mårmaglaciären and a resulting positive mass balance, it is possible that some snow will be added to the perennial snowfields at the end of the melt season.

According to the assumptions made the initial snow cover should have melted away in mid July in 1999, at the end of June in 1995 and at the end of July in 1993.

At first, the model was run with the parameters that were found to be optimal for Storglaciären (Hock, 1998), with MF 1.8 $mm^{-1}\ d^{-1}\ °C^{-1}$ and a_{snow} $0.6 * 10^{-3}$. The calibration was done separately for each year in order to find an optimal set of parameter where the melt rate seems reasonable according to the assumptions made. It is impossible to obtain total agreement in all four cirques, since two of the cirques have no measured snow cover. The calibration therefore focuses entirely on agreement in the cirques with measured initial snow cover, which is the eastern and central cirque (Figure 2).

In 1993, all cirques except the eastern cirque was free from snow on 29 July when using the parameters set for Storglaciären. Snow remains on the mountain ridge that is close to the eastern cirque even if the melt season was prolonged until October. In 1995 the snow disappears much earlier. In the beginning of June there is little snow left in all cirques. On 19 June, the eastern and the central cirque are snow free. In 1999 there is snow left in the cirques at the beginning of July but on 19 July they are free from snow (Figure 7).

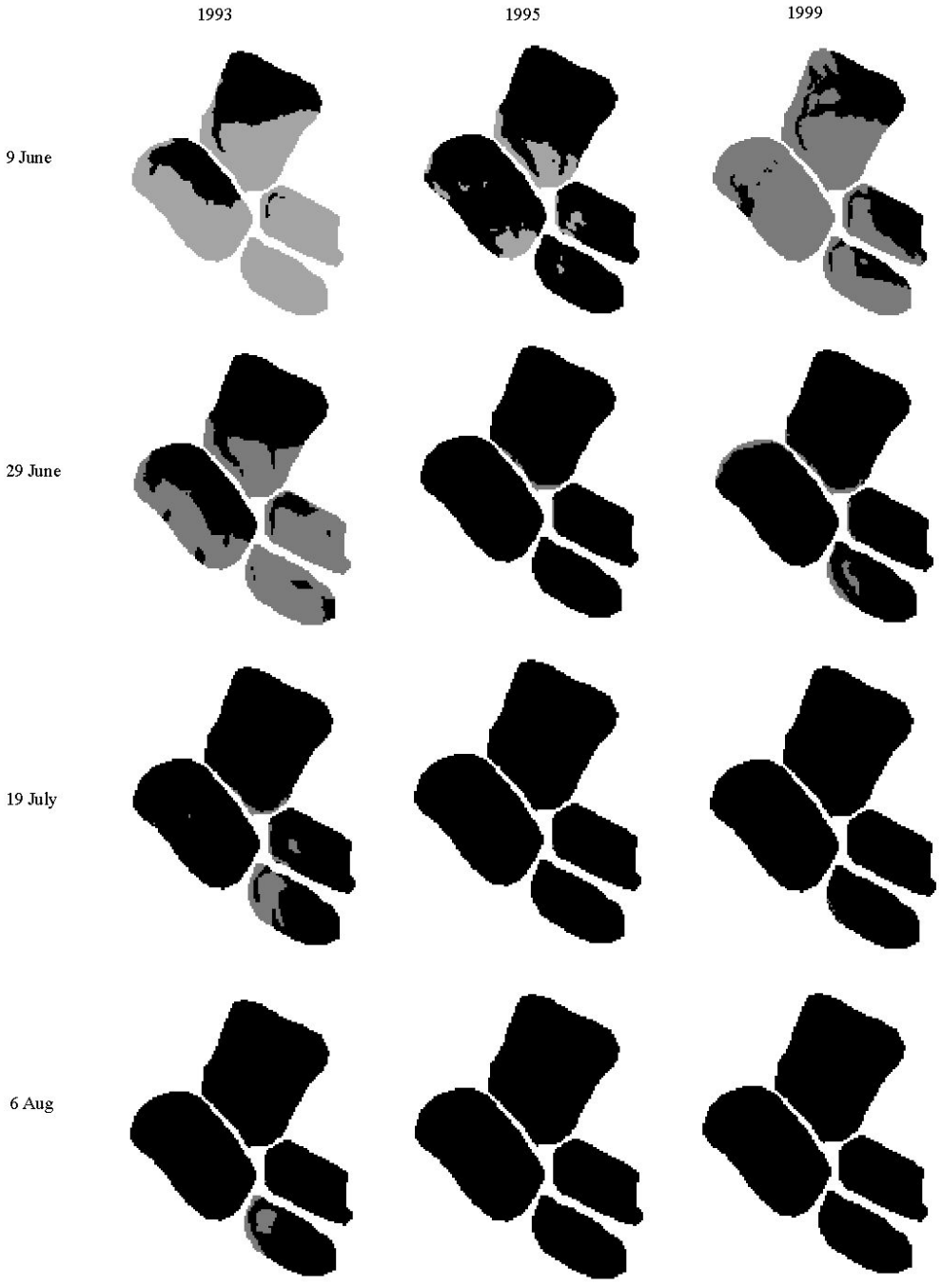

Figure 7. The remaining snow cover (grey) in the beginning of June, end of June, middle of July and beginning of August.

The diversity in the calculated ablation for the different years is due to the various amount of snow at the end of the winter seasons. One explanation of the different initial snow covers could be differences in the prevailing wind direction. Snowdrift often produces snow accumulation many times larger than those due to snowfall alone (Kind, 1981). However, the recorded weather data do not support this theory. The prevailing wind direction during the three years is the same, from S – SSE and NW (Figure 8). Another possible explanation might be the frequency of avalanches in the area. In 1993 it seems reasonable to assume that the frequency of avalanches was high, since the measured snow depth varied from 2 up to 10 m in the eastern cirque. In 1995 occurrence of avalanches have probably been less frequent since the amount of snow in same cirque was much less. If the snow has been exposed to a rapid rise in temperature the risk of avalanching increases (Schaerer, 1981). Meteorological measurements show that there was a rapid rise in temperature in 1993, just before the snow depth measurements were done. This event cannot alone explain the great amount of snow located in the eastern cirque in 1993 but it may have contributed to it. The measurements made in 1993 can have included measurements from the perennial snowfields, which also could explain the large amount of snow this year.

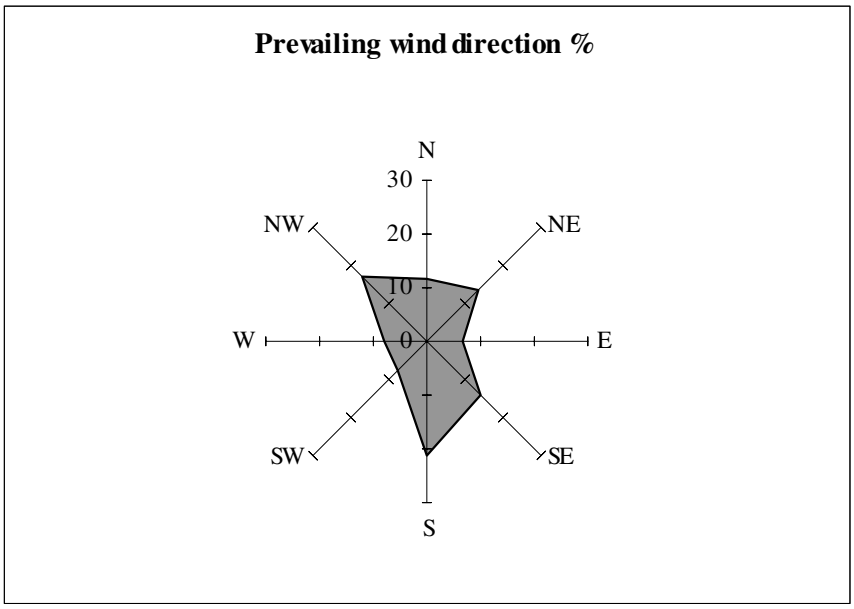

Figure 8. The prevailing wind direction in 1993, 1995 and 1999 in the Rassepautasjtjåkka massif.

Using the parameters for Storglaciären seems reasonable since the snow melts in the right sequence for the different years according to the assumptions made. In 1993 there will be snow left in the eastern cirque at the perennial snowfield and on the mountain ridge. But this is also according to the assumptions since the mass balance on Mårmaglaciären this year was unusually positive. By using these parameters, the spatial pattern of snowmelt was such that snow remained the longest near the perennial snowfield. The result from the calibration was thus in accordance with the assumptions and therefore no further calibration was needed.

The Degree-day factor (*DDF*) was calculated for all melt seasons, by dividing computed melt by the temperature (Equation 2). In 1993 the calculated *DDF* was 3.45 mm^{-1} d^{-1} $°C^{-1}$, in 1995 it was 3.55 mm^{-1} d^{-1} $°C^{-1}$ and in 1999 it was 3.34 mm^{-1} d^{-1} $°C^{-1}$. The average *DDF* in Rassepautasjtjåkka is 3.34 mm^{-1} d^{-1} $°C^{-1}$. In 1993 and 1994, climate stations were situated on Storglaciären and using data from these stations average *DDF* was calculated. The measured average *DDF* from a surface covered by snow was 3.2 mm^{-1} d^{-1} $°C^{-1}$ (Hock, 1999). Hock (1998) presented *DDF* for snow in non-glaciated areas and the values were ranging from 2.3 up to 7.5 mm^{-1} d^{-1} $°C^{-1}$. The measured *DDF* for snow from 12 non-glaciated areas in Finland was approximately 3.5 mm^{-1} d^{-1} $°C^{-1}$ (Kuusisto, 1980). The calculated *DDF* for Rassepautasjtjåkka are in agreement with both the measured *DDF* for Storglaciären and also with the *DDF* measured from non-glaciated areas in Finland.

5 Topographic effect on spatial distribution of potential direct solar radiation and snow melt

5.1 Results

The topographic effects on the distribution of potential clear-sky direct solar radiation and melt are large in the study area. The calculated direct radiation varies both temporally and spatially. The temporal differences are large even in a short time interval as a few hours. As an example we can review conditions during the 19th of June (Figure 9), which shows how the amount of potential direct radiation varies during a day. The available radiation varies from a few W/m^2 in the middle of the polar summer night up to 900 W/m^2 in the middle of the day. In late spring the temporal variations during a day is less, ranging from 0 up to approximately 650 W/m^2.

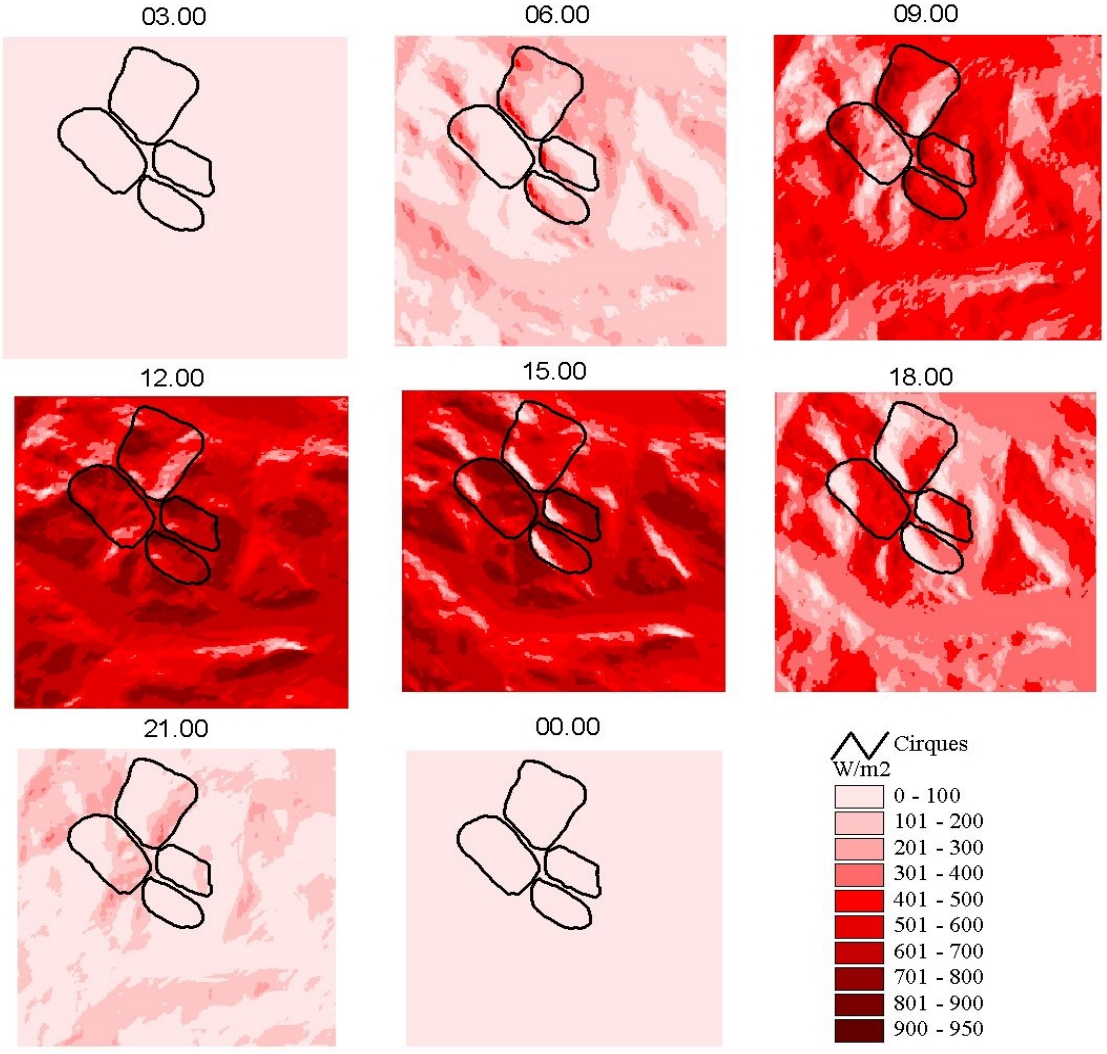

Figure 9. Diurnal variation in calculated potential clear-sky direct solar radiation during the 19th of June.

There are great spatial differences as well. In figure 9 the spatial differences during a day can be seen. In the morning the southwest-facing slopes are shaded and later in the day it is in general the north-facing slopes that are in shade. The spatial differences during a melt season, May to August, are very pronounced. The average potential clear-sky direct solar radiation was calculated for the period ranging from 61 to 297 W/m^2 in the Rassepautasjtjåkka massif.

To determine the topographic effects, a mean value for potential direct radiation was calculated assuming a flat topography and using the mean elevation for the study area, 1189 m a.s.l. The mean value was calculated for the period May-August. Since the slope and aspect were set to zero, no spatial differences occur in the calculated potential direct radiation yielding 234 W/m^2 for the site. A comparison between the calculation not including topographic effects and the one including topographic effects shows that excluding topographic effects both understates and exaggerates the potential clear-sky solar radiation (Figure 10). The calculated radiation on the south-facing slopes is understated and on the north-facing slopes it is exaggerated.

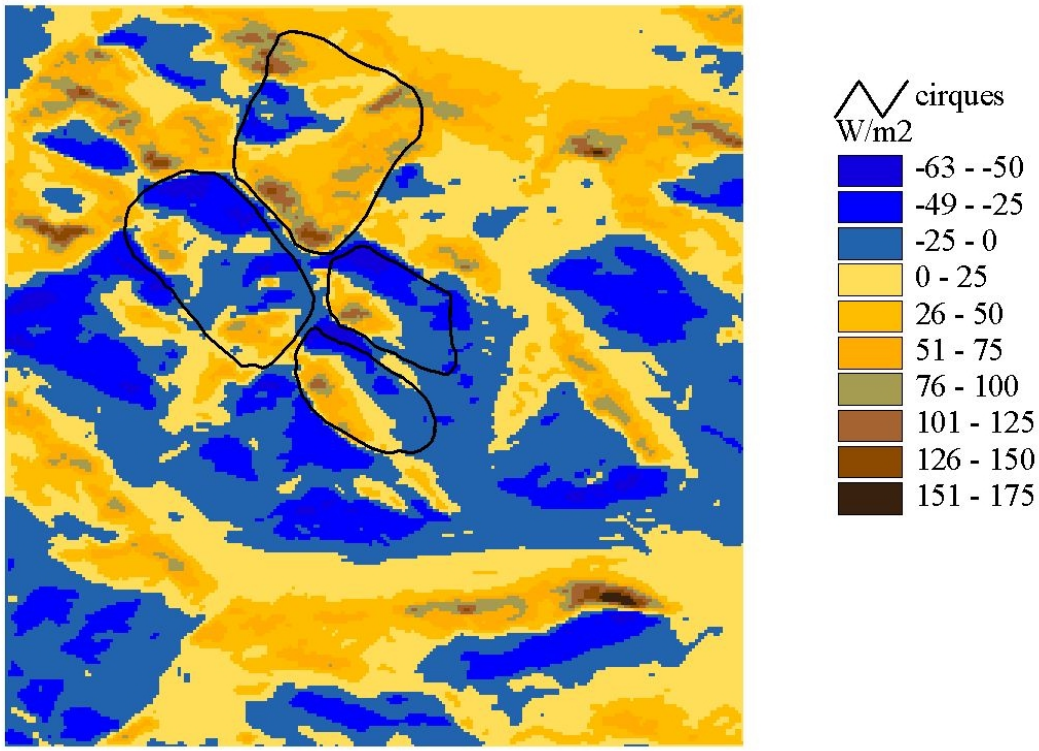

Figure 10. The difference in potential solar radiation between calculations including and excluding topographic effects. Calculations excluding topography underestimates the radiation on the south-facing slopes and exaggerates it on the north-facing slopes.

The climate station in the central cirque measures global radiation every third hour. The calculated potential clear-sky direct solar radiation is calculated every 15 minutes and a three-hours means are presented here. A comparison between the calculated radiation (direct radiation) and the measured global radiation (diffuse and direct) shows the same diurnal pattern (Figure 11). The seasonal pattern is easy to distinguish in the calculated radiation record for the period, May-August. The measured global radiation also increases during the day in the beginning of the season, but this trend declines after the middle of June. The potential direct solar radiation is highest at the summer solstice and then it decreases again towards the autumn.

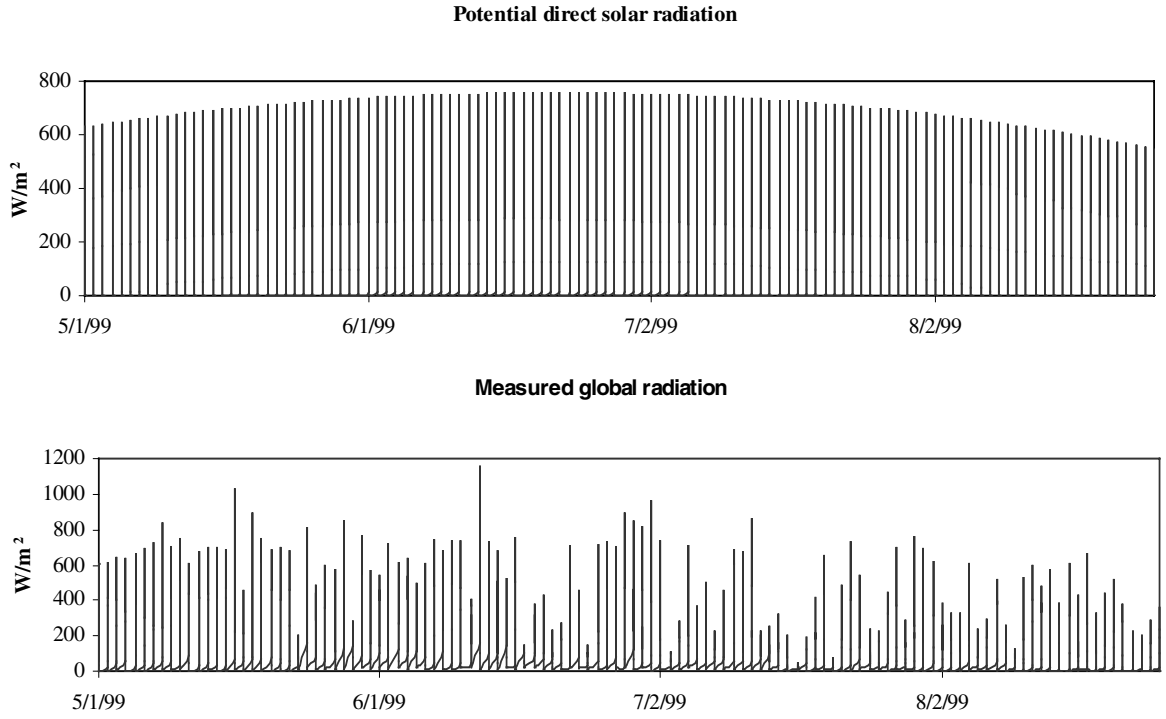

Figure 11. Calculated potential clear-sky direct solar radiation and measured global radiation at the climate station, during the period May-August 1999.

The topographic effects on melt rate follow the same pattern as the effects on the potential direct solar radiation. The accumulated melt for the period May-August, is ranging from 0.85 m w. eq., on the north-facing slopes to 2.68 m w. eq., on the south-facing slopes (Figure 12). A comparison between the calculations not including and including topographic effects show that the melt rate on the north-facing slopes are exaggerated by up to 0.85 m w. eq. and on the south-facing slopes the melt rate are underestimated by as much as 0.28 m w. eq., when excluding topographic effects.

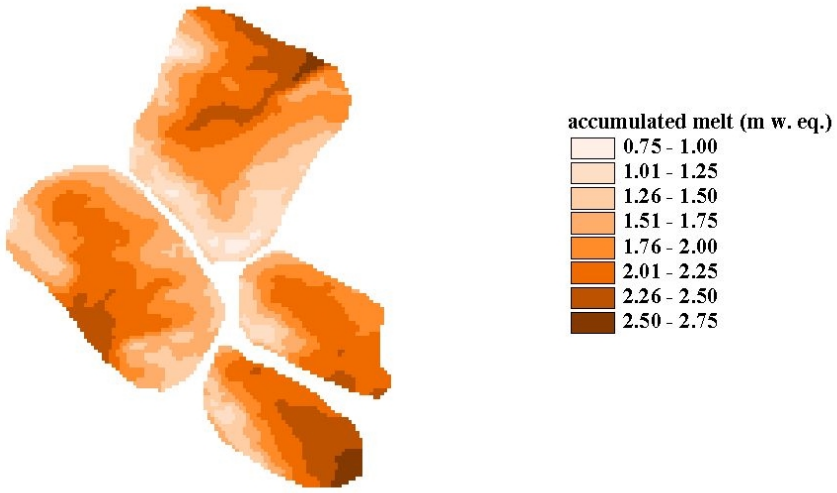

Figure 12. The influences of topography on the spatial distribution of snow melt.

5.2 Discussion

The potential direct solar radiation varies both seasonally and spatially. The seasonal variation occurs because the computed topographic shading is based on the position of the sun and the effective horizon. In figure 9 it is evident that potential direct radiation is present even during the night because the sun is very close to the summer solstice (which occurs the 21st of June). On this day the solar rays falls more directly on the Northern Hemisphere than any other day and the areas in the Artic circle, which is the case with the study area, have daylight that lasts for 24 hours. More crucial to the seasonal and diurnally changes are though the slope angle and aspect in the area.

The spatial differences calculated for the whole period, ranging from about 60 to 300 W/m^2 are similar to the spatial differences calculated for Storglaciären during a melt season. On Storglaciären the value was ranging from less than 50 up to 250 W/m^2 (Hock, 1998). The spatial differences in potential direct radiation when including and excluding the topographic effects are to a great extent determined by the point of the compass, with exaggerated north-facing slopes and underestimated south-facing slopes.

Figure 11 shows that the diurnal pattern is similar for both the calculated and the measured global radiation. The seasonal variation in the direct radiation is easy to distinguish. In the measured global radiation record it is hard to detect a seasonal change, because of the effect of cloud cover in the study area. This is especially pronounced from mid-July probably due to an increase in cloud cover and more frequent cyclones in the study area. The cloud cover affects the short-wave radiation and the amount of global radiation that reaches the earth's surface is decreased. In a longer period the seasonal variation would be distinguishable even in the measured global radiation since there are great difference in the amount of solar radiation available during summer and winter.

The global radiation significantly affects the melt rate in the Rassepautasjtjåkka massif which is in accordance with Oerlemans *et al* (1999) and Ohmura *et al* (1992) conclusion that the global radiation is a major source of melt. Because the elevation ranges from 1080 to 1728 m.a.s.l. and the walls forming the cirques are very steep, the spatial differences in melt are especially pronounced in the study area. Since the topographic effects of melt are large in the area it is important to include them when calculating the melt. In contrast to the model used in this study, the ordinary degree-day model does not take into account any spatial or temporal differences in melt. The fact that an ordinary degree-day model does not take any topographic shading or decreasing energy during night into account does make the result from a degree-day model debatable.

6 Conditions for re-glaciation

6.1 Results

Under present climate conditions after a melt season, snow remains in the cirques only in certain years. The calibration showed that the initial snow cover melts away unless there is an unusually large accumulation volume at the beginning of the melt season. The summer melt conditions, in this case the temperature and the potential clear-sky direct solar radiation, determines the maximum amount of snowmelt during a melt season (May - August). To determine the amount of snow that could potentially be melted under the present climate conditions if the snow supply was unlimited a model run was done assuming a 10 m initial snow cover, which is equivalent to 3.5 m w. eq., for the whole area. The total amount of melt varies between years (Table 5). The potential melt-capacity within the study area, varying because of effects from the surrounding topography, ranged from 0.93 to 3.02 m w. eq., in 1993.

Table 5. The accumulated snowmelt during a melt season May – August.

Year	Total amount of melt m^3 w. eq	Average melt m w. eq.
1993	15 705.5	2.08
1995	17 230.3	2.29
1999	13 850.8	1.84

Two climate variables can be changed to determine the climate conditions required to re-glaciate the cirques in the Rassepautasjtjåkka massif. These are winter precipitation (changing the amount of snow at the beginning of the melt season) and temperature. At first, each variable was changed under otherwise equal conditions. Later a combination of changing both parameters was done in order to determine the optimal parameter. The following climate scenarios were used:

- Decreasing the temperature by 1, 2, 3, 4 and 5°C
- Increasing the initial snow cover by 50, 100, 150, 200 and 250%
- Decrease the temperature and increase the initial snow cover by 1°C and 50%, 2°C and 50%, and also by 1°C and 100%

As input to the model when running different climate scenarios, an initial snow cover file was used, containing the average of the three measured initial snow covers. The climate file to be used was that from 1993, since the potential melt rate this year was less then 1995 but larger than 1999.

Under present climate condition and using the input file containing an average of the measured initial snow covers no snow remained after a melt season. A decrease in temperature by 2-3 °C from prevailing temperature will result in snow remaining after a melt season (Figure 13). Under these conditions snow is added on the perennial snowfield in the eastern cirque and on the mountain ridge as well. There are great differences between the amount of remaining snow cover when decreasing the temperature by three and four degrees, respectively. The number of occasions when melt occurs (temperature above 0°C) is lowered from 483 to 405 occasions. If temperature was decreased by 5 °C compared to present temperature there was snow left in approximately $^1/_3$ of each of the four cirques. The amount of snow varied from 0.01 up to 1.34 m w. eq.

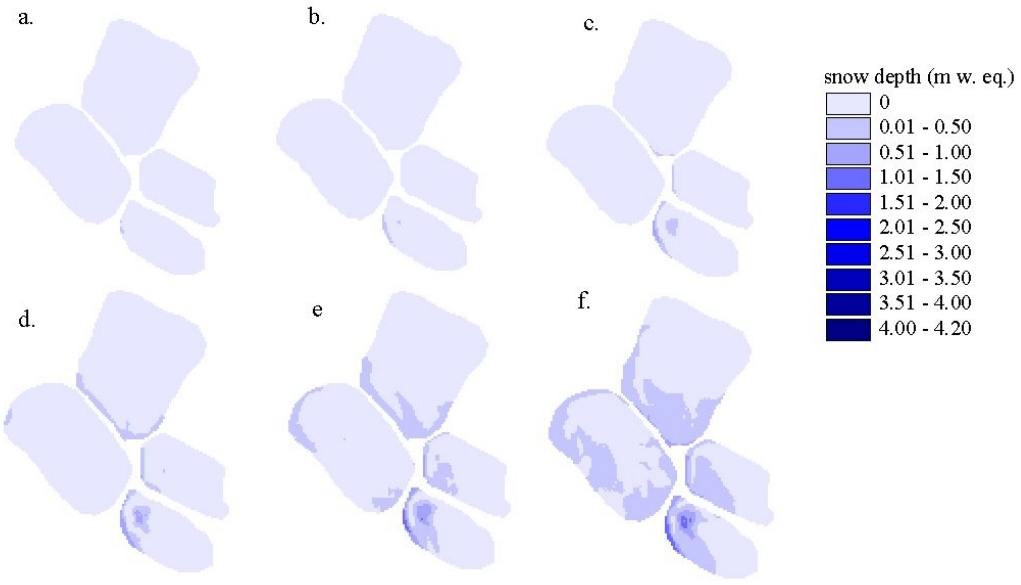

Figure 13. Remaining snow cover after a melt season under present conditions (a), when decreasing the temperature by 1 °C (b), 2 ° C (c), 3 °C (d), 4 °C (e) and 5 °C (f).

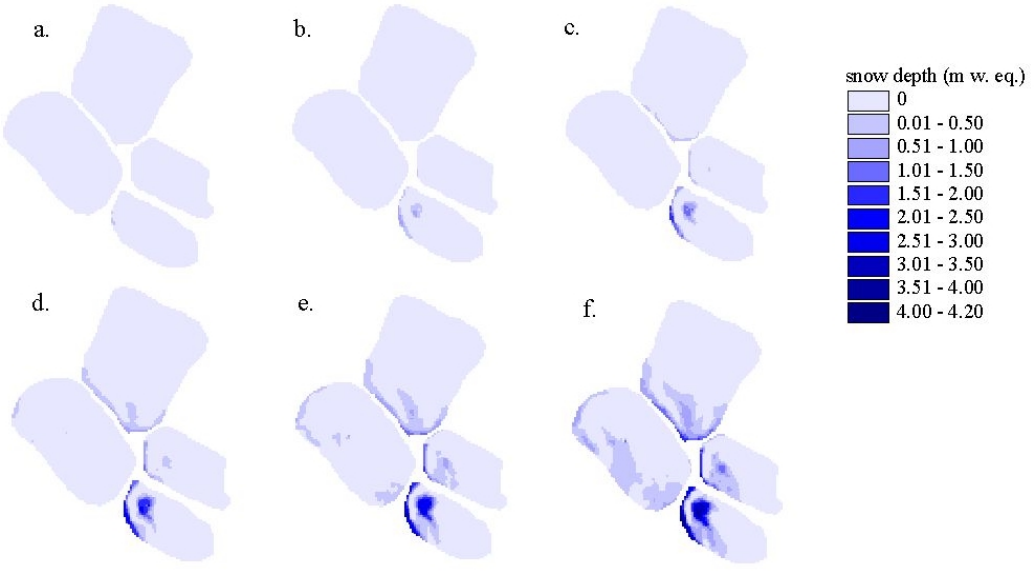

Figure 14. Remaining snow cover after a melt season under present conditions (a), when increasing the initial snow cover by 50% (b), by 100% (c), by 150% (d), by 200% (e) and by 250% (f).

When adding 50% more snow to the existing initial snow cover, there was a small amount of snow left at the perennial snowfield in the eastern cirque (Figure 14). By adding 150% more snow there was a small amount of remaining snow cover in all four cirques, dominating on the mountain ridge. When increasing the initial snow cover with 250% approximately ¼ of the

central and eastern cirques was covered by snow. The other cirques were also snow covered but to a lesser extent. The remaining snow cover, when increasing the initial snow cover by 250%, covered a smaller area than when decreasing the temperature by 5 °C. The total area that is covered by snow is 4.85 km^2 when adding 250% more snow and when decreasing the temperature the area is 6.83 km^2. A larger amount of snow is though left in the cirques in the first scenario (Figure 13 and 14).

A climate scenario that includes both a temperature decrease during summer and an increase of initial snow cover was used. This corresponds to a more maritime climate, which usually implies colder summer and milder winters with increased precipitation. By changing both parameters a more realistic answer to the question of what climate conditions are required for making a re-glaciation in the empty cirques possible, might be found. At first, the temperature was lowered by 1 °C and the initial snow cover was increased by 50%. Snow remaining after the melt season was only present in the eastern cirque and on the mountain ridge separating the four cirques. When the temperature was decreased by 2 °C and the initial snow cover is still increased with 50%, the result is different. Under these conditions snow occurs in all four cirques after a melt season and can form the basis for building a glacier (Figure 15). When increasing the initial snow cover by 100% and lowering the temperature by 1 °C, the same pattern as in the previous example was found. However a larger area is covered by snow (1.38 km^2) compared to when the temperature was lowered by 2 °C and 50% more snow was added (1.32 km^2).

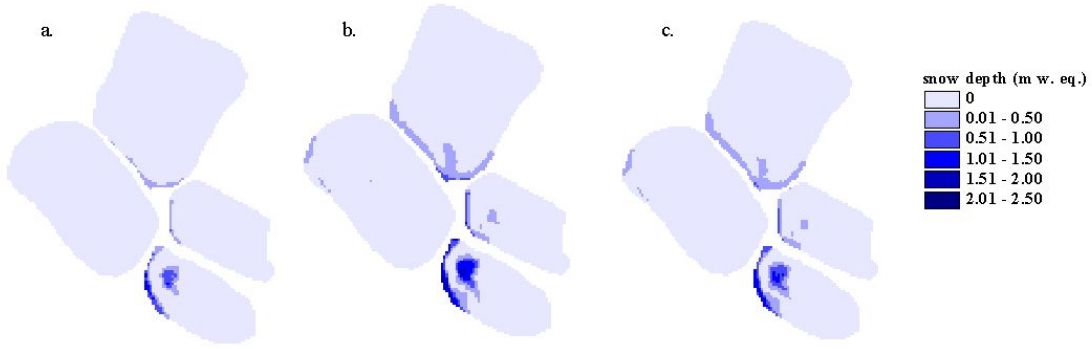

Figure 15. Remaining snow after a melt season: when decreasing the temperature by 1°C and increasing initial snow cover 50% (a), decreased temperature by 1 °C and increased snow cover by 100% (b), decreased temperature by 2°C and increased snow cover by 50% (c).

6.2 Discussion

6.2.1 Conditions for re-glaciation

The result from the climate scenarios shows that the melt conditions in the Rassepautasjtjåkka massif, when varying the input parameters are sensitive to a climate change. The summer temperature alone needs to be lowered by 2-3 °C before there will be snow left in the cirques after a melt season. Jansson *et al* (1999) concluded that a moderate temperature change is necessary to initiate a glaciation in the empty cirques but that a decreasing temperature would lead to a cold-based glacier. In a cold-based glacier the basal temperature has not reached pressure melting point and there is no movement in the basal region. Since there is no basal

movement there will not be any erosion and the cirques could not have been eroded under these climate conditions (Hooke, 1998). To get a warm-based erosive glacier Jansson *et al* (1999) concluded that a higher winter precipitation was needed and also warmer winter temperature. If a decrease in summer temperature by 2 - 3 °C is a result of a more maritime influence on the climate then the winter temperature might increase.

An increase in the winter precipitation (increase initial snow cover) by 50 – 100 % will result in some remaining snow in the cirques. By adding 250% more snow there will be a great amount of snow left in the cirques. This however would not result solely in glaciers in the cirques, since there would be snow left in the surroundings as well. The winter climate in northern Scandinavian is governed by the location of the polar front. A more northerly location of the polar front would lead to more winter precipitation (Jansson *et al*, 1999).

When combing the two parameters, snow is left when decreasing temperature by 2°C and adding 50% more snow and also when the temperature is decreased with -1°C and 100% more snow is added. Schneeberger (1998) investigated how Storglaciären would react to a possible climate change. It is interesting to note his choice of climate scenario, a small warming defined as 1°C combined with a high increase in precipitation, which was 20% per degree warming. A comparison with the relationship between increased temperature and increased precipitation used on Storglaciären and how this would affect the temperature in Rassepautasjtjåkka is of interest. Using Schneeberger's high increase in precipitation 20 % per degree warming, the 50% added snow would require an increase in temperature by approximately 2.5°C. Including the decreased summer temperature by 2°C inferred to be the optimal scenario would require a climate that was much more influenced by maritime conditions than the current. To achieve a more maritime climate annual temperature amplitude must be decreased, the westerlies must be induced and generate higher winter precipitation. This climate conditions occurs when the NAO index shows a positive phase. The NAO index has been positive since the 1970s and especially positive from late 1980s to 1994-1995. In the winter 1995/1996 the index reversed its sign and in many parts of Europe this winter was the coldest for at least 10 years and it was also a very dry winter in northern Europe (Jones *et al*, 1997).

It is hard to determine how long it would take to build a glacier, partly because the melt conditions in the study area is not completely known, but also because of the positive feedback that occurs when snow is added to the perennial snowfields. For example the melt rate will be reduced because the remaining snow will change the albedo and will increase the reflectance of global radiation, which is known as a major source of melt. After a while, when the snow pack has become quite thick, the decreasing temperature with increasing height would also have a minor effect on the snowmelt. Another thing that make it complicated to determine how long a re-glaciation would take is that the model used does not take into account precipitation during summer. Summer precipitation in terms of snow would speed up the process while summer precipitation in terms of rain would result in additional source of heat to the snow pack. This however would only enhance the melting process marginally.

6.2.2 Comparison with proxy data from the Holocene

Based on the geomorphology in the study area, Jansson *et al* (1999) concluded that there has not been any glaciation in the empty cirques during the Holocene. To see whether the climate conditions suitable for a re-glaciation in the cirques have occurred during the Holocene proxy data have been used.

There are however problems connected to dating proxy-data and that is that the age specified can be quite uncertain. Analyses from ice-cores drilled on Greenland (Camp Century) shows that this last millennium has been colder than the six previous ones. The climate was found to be especially warm between 4000 and 6000 years ago, in contrast the beginning of Younger Dryas was very cold (Dansgaard, 1984). Proxy data of this kind gives a general picture of the climate during the Holocene in the Northern hemisphere.

The regional climate in northern Europe during the Holocene is inferred from studies of marine sediment cores. Hass (1996) concluded that the climate in northern Europe around A.D 400-600 was characterized by increased moisture and decreasing temperature. In A.D 800, 1000-1300 and 1500 temperature was in average 0.5-2 °C higher than the current conditions, with warm summers and mild winters. 1500-1800 was the coldest period since Younger Dryas and the temperature dropped 1-2 °C below present (Hass, 1996).

In order to reveal the climate conditions that occurred in northern Sweden during Holocene proxy data like glacier advances, pollen analyses and tree-ring records from this region was used. Barnekow (1999) reconstructed the Holocene vegetation history and climate changes in the sub-artic area in Northern Sweden, Abisko (Figure 1). The study is from present until 10 000 BP. The vegetation history is based on pollen and macro fossil analyses from six lakes. Major parts of the Abisko area were deglaciated around 10 000 BP and some dead ice remained until 9100 BP. In general an expansion of boreal ecosystems during the Holocene seem to reflect increased temperature and humidity. Mountain birch is favoured by a cool-humid (snow rich) climate with relatively small seasonal contrast (maritime climate) while Scots Pine is adapted to more continental conditions i. e. warm and dry summers and a sparse winter snow-cover (Kullman, 1992). Barnekow has used those types of trees to determine the climate conditions.

Karlén (1982, 1988) has put together information about glacier fluctuations in Scandinavia from historical records, radiocarbon dating on moraines, lichenometric dates on moraines and from changes in the composition of lacustrine sediments in lakes located down stream from glaciers. There have been many periods during Holocene when glaciers have been reported to advance and grow. The more pronounced advances that are known in Scandinavia occurred about 7500, 5100-4500, 3200-2800, 2900-2200, 1500-1100 and 350-20 BP. An attempt to compile the information that is collected from Karlén and Barnekow is done in figure 16.

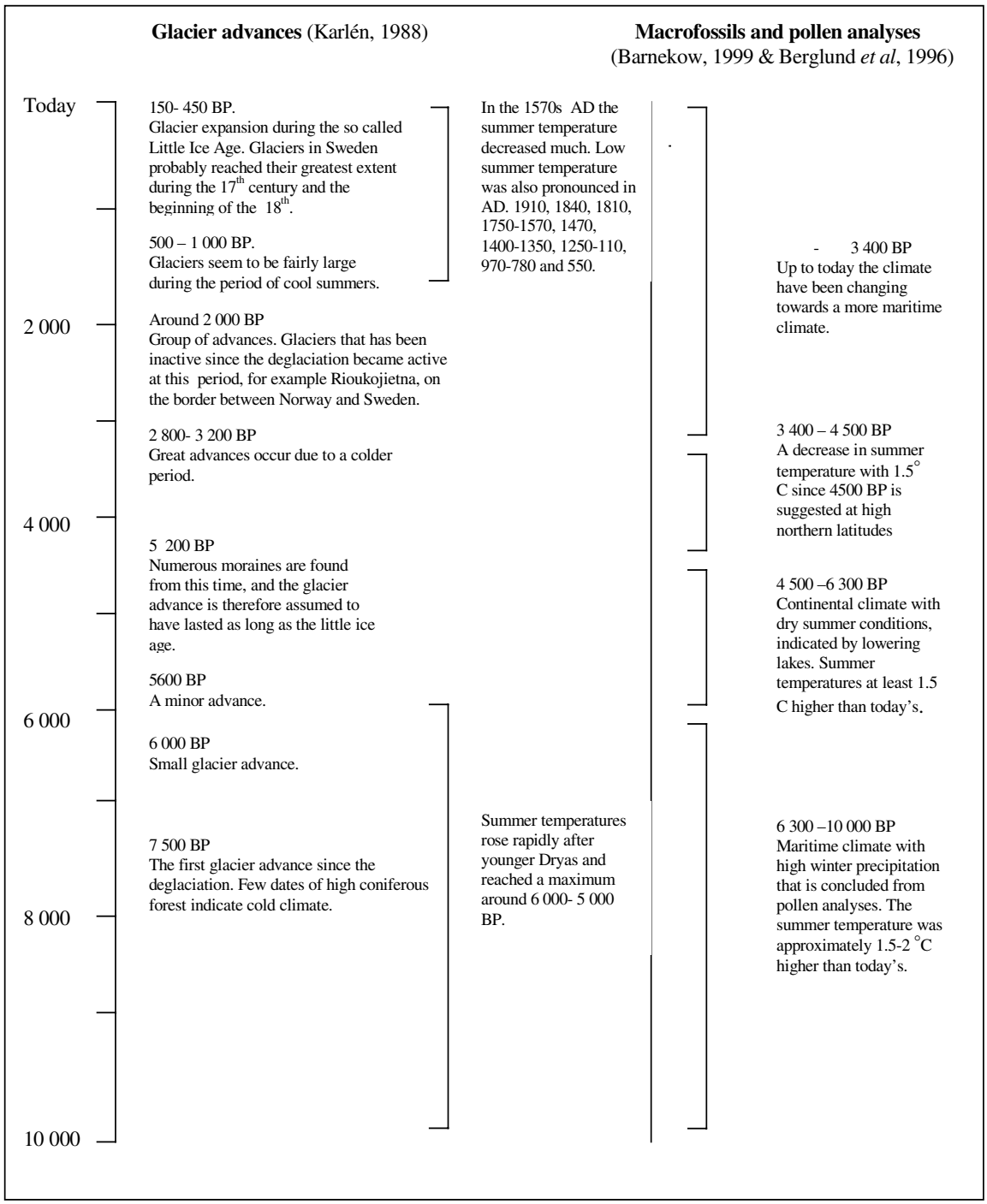

Figure 16. Proxy data derived from glacier advances in northern Sweden and Norway (Karlén, 1988) and also from pollen and macrofossils analyses in Torneträsk area, northern Sweden (Barnekow, 1999).

At Mikkaglaciären northern Sweden, the outermost Holocene moraines are dated from about 3700 BP (Karlén and Denton, 1975). During the Holocene there were fairly long colder periods in northern Scandinavia, definitively long enough for the glacier to reach its maximum (Mörner and Karlén, 1984). If the winter precipitation would have been similar to present conditions then Mikkaglaciären should have been much larger than the area represented by the outermost moraines (Holmlund, 1986). Holmlund (1986) therefore assumed that the winter precipitation was reduced during these cold periods. One explanation might be less cyclonic storm activity due to colder winters. Less precipitation means a more continental climate than present (Holmlund, 1986).

The most recent report of advancing glaciers in Scandinavia was between the 16th and the 20th century (Karlén, 1982). In the middle of the 16th century a pronounced climate change occurred. The coldest period since the last ice age ended was a fact until the middle of the 18th century. During this period there were great variations from year to year and also from one group of a few year to the next. Observations from the late 16th century, Tycho Brahe from Denmark implied that the winter temperature was about 1.5 °C lower than in modern time. The easterly winds were reported to be more prominent. Glaciers were reported to overrun farms and farmland in Scandinavia in the late 17th century (Lamb, 1995).

Using tree-ring records the temperature during the major part of the last millennium in northern Fennoscandia is derived. Briffa *et al*. (1992) reconstructed the summer temperature in Fennoscandia to extend back 1400 years based on tree-ring record. They plotted the temperature as anomalies from the mean 1951-1970, which showed that periods of generally cool and generally warm conditions are typical of northern Fennoscandian summers throughout the last millennium (Table 6).

Table 6. The extreme summer temperature (April-August) as anomalies from the mean 1951-1970, found in the northern Fennoscandian record (Briffa et al., 1992).

50-Year means			
Positive		Negative	
Period	Anomaly (°C)	Period	Anomaly (°C)
1402-1451	0.54	1576-1625	-0.67
1043-1092	0.52	1632-1681	-0.49
957-1006	0.44	638-687	-0.42
745-794	0.35	1108-1157	-0.37
886-935	0.24	1862-1911	-0.32

During the latest millennium cold periods have occurred in the early 7th and 8th century, in the middle of the 12th century and the longest period of colder summer temperature is found in the late 16th until the end of the 18th century. The warmer period was found in the early 15th century that was as warm as the 10th and 11th and the present century (Figure 17) (Briffa et al., 1992). Based on glacier advances and ^{14}C-dated samples Karlén and Kuylenstierna (1996) also concluded that during the 1800s, the average summer temperature in northern Scandinavian was close to the 1°C colder than in 1940. During the 1700s century the temperature was only slightly colder but probably due to a longer period it resulted in more extensive glacier advances (Karlén and Kuylenstierna, 1996). Out of the proxy-data presented here the climate conditions during the Holocene is summarized in table 7.

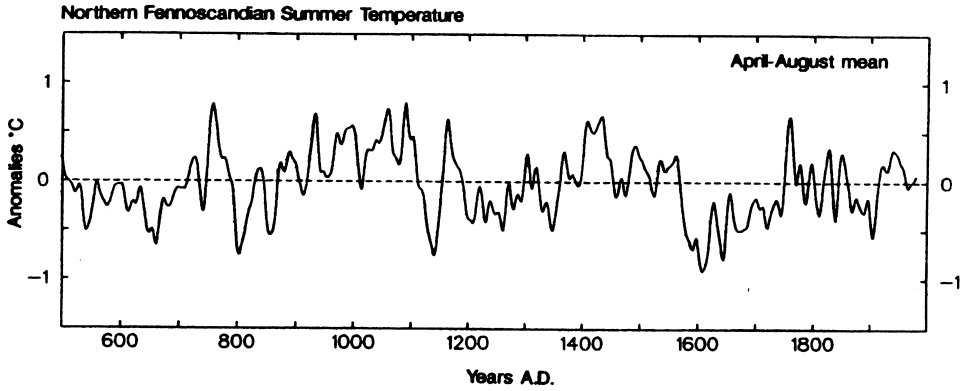

Figure 17. Temperature derived from dendro-chronology extending 1400 years back (Briffa et al., 1992).

Table 7. Climate conditions during Holocene derived from proxy-data.

Year (BP)	Temperature	Precipitation	Comments
11 000 - 10 000	Colder than present	--	This period is defined as a very cold period, 10 000 BP major part of the area was deglaciated.
10 000 - 6 000	1.5 - 2°C warmer summer temperature than present	High winter precipitation	Glacier advances occurred in the middle and end of the period
6 000 - 4 000	Summer temperature 1.5- 2°C warmer than present	Dry summer conditions	This period is defined as especially warm.
4 000 - 3 000	Summer temperature 1.5 °C lower than the temperature found 4 500 BP	Less precipitation	A more continental climate than present
3 000 – 1 500	--	--	Climate changing towards a more maritime climate, followed by glacier advances
1 500 - 1 000	Periods of lower summer temperature, at the most 0.6 °C lower than present	Increased moisture in the beginning of this period	Glaciers are fairly large during the periods with cold summers
1 000 - 500	Generally warm and generally cool summers	--	1 000, 700 and 500 BP the northern Sweden experienced warm summers and mild winters
500 - present	Temperature –1 °C colder than present	--	Coldest period since the Younger Dryas, glacier in Sweden reached probably their greatest extent.

The climate required to get a re-glaciation in the empty cirques in the Rassepautasjtjåkka massif is either a decrease in temperature by 1 °C in combination with an increase in initial snow cover by 100%, or a decrease in temperature by 2 °C together with an increase in snow cover in the beginning of the melt period by 50%. Glaciers have advanced during several periods during the Holocene. According to the proxy data the most favourable conditions for a re-glaciation would be during the 15th to the beginning of the 20th century when the coldest period since the Younger Dryas occurred and many glaciers in Scandinavia advanced to their maximum extent, but there are no signs of glaciation in the cirques during this period. This conclusion is based on the fact that the summer temperature was only 0.5 °C lower than present and the periods was not lasting long enough. Another fact that points towards that there have not been any glaciers during the period referred to as the "Little Ice Age" is the absence of trim lines (i. e. vegetation boundaries that follows a retreat of a glacier and reflects the former position of the ice surface) in Rassepautasjtjåkka massif (Jansson *et al*., 1999). These features correspond to the "Little Ice Age" advance that is almost equal to the maximum extent of postglacial glaciation (Karlén, 1982). During the Holocene the colder periods and increased precipitation has not occurred at the same time, rather a decreased precipitation has occurred at the same time as colder periods. Since the calculated climate scenarios requires both lowered temperature and increased precipitation the climate conditions required for a re-glaciation have not been found in the climate data from the Holocene it can be concluded that there has not existed any glaciers during Holocene in the empty cirques in the Rassepautasjtjåkka massif.

7 Future scenario

7.1 Results and discussion

Since the theoretical climate conditions required to glaciate the cirques are already determined, I will only briefly present how a possible future climate scenario, predicted for the region by climate models, can affect the melt conditions and remaining snow cover in the cirques in the Rassepautasjtjåkka massif. The Swedish Meteorological and Hydrological Institute, SMHI, in cooperation with the Universities of Gothenburg and Stockholm studies regional climate scenarios in Sweden in a project called SWECLIM. They also predict future climate in Sweden based on a regional climate model (Räisänen *et al.*, 1999). The precipitation is predicted to increase by 30-40% until 2100. The increase will occur during all seasons but is largest in summer and autumn. The temperature is predicted to increase between 4 and 5 °C in the northern part of Sweden. By using a climate scenario that can be compared to the one that SWECLIM have predicted a possible future melt rate could be visualised. The climate scenario that was used contained an increased winter precipitation by approximately 20% (since the increase is less in the winter) and an increase in temperature by 4 °C (Räisänen *et al.*, 1999).

The total amount of snow that could be melted when increasing the annual average temperature by 4 °C was calculated by using an initial snow cover that was 30 m thick (10.5 m w. eq.). The average accumulated melt rate in the cirques, during the period May-August, is then 4.05 m w. eq., which can be compared to existing climate conditions when the average accumulated snow melt in the cirques is approximately 95% less (2.08 m w. eq.). The increase in temperature by 4 °C increased the melt rate, and even if 20% precipitation was added to the initial snow cover, the result indicated that the snow would melt away earlier than today. The melt season would be prolonged since there were more days that had temperatures above zero later in the season. A re-glaciation in the empty cirques in the near future according to this climate scenario is therefore eliminated.

The same future climate scenario has been used to predict how existing glacier will react on a climate change. Oerlemans *et al.* (1999) have calculated possible changes in the mass balance of Storglaciären (Tarfala) (Figure 1) and Nigardsbreen (Norway). The predicted temperature change is larger for Storglaciären than for Nigardsbreen. The increasing temperature affects the mass balance negative and the increasing precipitation affects the mass balance positive. The increase in precipitation compensates only a small part of the increase in melt. Calculated annual total of the mass balance showed that both Storglaciären and Nigardsbreen was loosing approximately 1 m w. eq. a^{-1} (Oerlemans *et al.*, 1999).

The Intergovernmental Panel on Climate Change, IPCC (Kattenberg *et al.*, 1996), produce future climate scenarios on a global scale and the primary emission scenarios used are called IS92. This prediction is in accordance with that from SWECLIM. The temperature increase will vary between 1.25-2.3 °C, depending on different IS92-scenarios, and precipitation will increase during winter at high latitudes. Those future climate scenarios would result in that snow would disappear from the cirques earlier than today but not as early as when using the climate scenario predicted by SWECLIM. In either case the climate conditions required to get a re-glaciation does not exist.

8 Conclusions

- The topographic effect on the spatial distribution of the potential direct solar radiation and melt is of great importance in the study area. When using a classical degree-day model the spatial and temporal variation of melt is neglected and the melt capacity on a south-facing slope will be underestimated, while on the north-facing slopes it will be overestimated.

- The climate conditions that are required to get a re-glaciation in the empty cirques in Rassepautasjtjåkka are a combination of decreasing temperature and increasing precipitation. By either decrease the temperature by 2 °C and increase the initial snow cover with 50% or lower the temperature by 1 °C and add 100% more snow compared to current conditions, there will be snow left after a melt season in the cirques and this could constitute the base to a new glacier.

- The climate conditions that are determined to be optimal for a re-glaciation in the cirques have most likely not occurred during the Holocene. This assumption is based on proxy data derived from glacier advances, macrofossil and pollen analyses in northern Sweden.

- Since the optimal climate conditions has not likely occurred during Holocene, the origin of the cirques in the Rassepautasjtjåkka massif can be concluded to extend further back in time than Holocene.

- Even though the climate in Scandinavian can be said to have been favourable for glacier growth the last decades, the climate scenarios that is predicted in the future by the climate model from SWECLIM makes the likelihood of initiating a glacier in the near future unrealistic.

- The question how come there are glaciers situated so close to the Rassepautasjtjåkka massif and not in the massif still remains unanswered, but different regional gradient and local conditions that governs the precipitation probably contribute to it.

9 References

Alt, B. T., 1987: Developing synoptic analogs for extreme mass balance conditions on Queen Elizabeth Island ice caps. *Journal of Climate and Applied Meteorology* **26**, 1605-1623.

Barnekow, L., 1999: Holocene vegetation dynamics and climate changes in the Torneträsk area, northern Sweden. *Lundqua* thesis **43** Lund University, Department of quarternary Geology.

Berglund, B. E., Barnekow, L., Hammarlund, D., Sandgren, P. and Snowball, I. F., 1996: Holocene forest dynamics and climate changes in the Abisko area, northern Sweden – the Sonesson model of vegetation history reconsidered and confirmed. *Ecological Bulletins* **45**, 15-30.

Blösch, G., Kirnbauer, B. and Gutknecht, D., 1991: Distributed snow melt simulations in an Alpine catchment 1. Model evaluation on the basis of snow cover patterns. *Water Resources Research* **27**, 3171-3179.

Blösch, G. and Kirnbauer, B., 1992: Analysis of snow cover patterns n a small alpine catchment. *Hydrologic Processes* **6**, 99-109.

Bodin, A., 1994: Mass balance of Mårmaglaciären 1992/93. *Forskningsrapport* **100**. Jansson, P. Ed. Department of Physical Geography, University of Stockholm. 10-11.

Bonham-Carter, G. F., 1997: *Geographic Information systems for geoscientist, modelling with GIS*. Pergamon/Elsevier Science Publications, Canada. 398 pp.

Briffa, K. R., Jones, P. D., Bartholin, T. S., Eckstein, D., Schweingruber, F. H., Karlén, W., Zetterberg, P. and Eronen, M., 1992: Fennoscandian summers from from A.D. 500: temperature changes on short and long timescales. *Climate Dynamics* **7**, 111-119.

Dansgaard, W., 1984: Grönlandisen minns klimat och vulkanutbrott. *Forskning och framsteg* **4**, 4-12.

Eastman, J. R., 1997: *Idrisi for windows – User´s guide*. Clark Labs, Clark university, USA.

Eklundh, L. and Mårtensson, U., 1995: Rapid generation of Digital Elevation Models from topographic maps. *International Journal of Geographical Information Systems* **9**, 329-340.

Golding, D. L., 1974: The correlation of snowpack with topography and snow melt runoff on Marmount Creek basin, Alberta. *Atmosphere* **12**, 31-38.

Grove, J. M., 1988: *The little Ice Age*. Menthuen, London. 498 pp.

Grudd, H., 1990: Small glaciers as sensitive indicators of climatic fluctuations. *Geografiska Annaler* **72A**, 119-123.

Grudd, H. and Schneider, T., 1996: Air temperature at Tarfala research station 1946-1995. *Geografiska Annaler* **78A**, 115-119.

Hagan, J. E., Eastman, J. R. and Auble, J., 1998: *Cartalinx, The spatial data builder- Users guide.* Clark Labs, Clark University, Massachusetts. 197 pp.

Hass, H. C., 1996: Northern Europe climate variations during Holocene: evidence from marine Skagerrak. *Palaeogeography, Palaeoclimatology, Palaeoecology* **123**, 121-145.

Hock, R., 1998: Modelling of glacier melt and discharge. *Zurcher Geographische Schriften* **70**. 140 pp.

Hock, R., 1999: A distributed temperature index ice and snow melt model including potential direct solar radiation. *Journal of Glaciology* **45**, 101-111.

Hoinkes, H. C., 1968: Glacier variation and weather. *Journal of Glaciology* **7**, 3-19.

Holmlund, P., 1986: Mikkaglaciären: bed topography and reponse to 20th century climate change, *Geografiska Annaler* **68A**, 291-302.

Holmlund, P., 1987: Massbalance of Storglaciären during the 20th century. *Geografiska Annaler* **69A**, 439-447.

Holmlund, P., 1990: Cirques at low altitude need not necessarily have been cut by small glaciers. *Geografiska Annaler* **73A**, 9-16.

Holmlund, P., Karlén W. and Grudd, H., 1996: Fifty years of mass balance and glacier front observation at the Tarfala Research station. *Geografiska Annaler* **78A**, 105-114.

Hooke, R. LeB., 1998: *Principles of glacier mechanics*. Prentice Hall, New Jersey. 248 pp.
Hurrell, J. W., 1995: Decadal trends in the North Atlantic Oscillation and relationships to regional temperature and precipitation. *Science* **269**, 676-679.
Jansson, P., Jonsson, S. and Huss, E., 1994: Studies of local climate in empty glacier cirques located just below the glaciation limit. *Forskningsrapport* **100**. Jansson, P. Ed. Department of Physical Geography, University of Stockholm, 28-30.
Jansson, P. and Jonsson, S., 1996: Studies of local climate in empty glacier cirques located just below the glaciation limit - progress report 1995. *Forskningsrapport* **103**. Jansson, P. Ed. Department of Physical Geography, University of Stockholm, 30-31.
Jansson, P., Richardsson, C. and Jonsson, S., 1999: Assessment of requirements for cirque formation in northern Sweden. *Annals of Glaciology* **28,** 16-22.
Jones, P. D., Jonsson, T. D. and Wheeler, D., 1997: Extension to the North Atlantic Oscillation using early instrumental pressure observations from Gibraltar and south-west Iceland. *International Journal of Climatology* **17**, 1433-1450.
Jonsson, S., 1981: *Glaciologi* (kompendium). Department of Physical Geography, University of Stockholm.
Jonsson, S. and Jansson, P., 1993: Studies of local climate in empty glacier cirques located just below the glaciation limit. *Forskningsrapport* **96**. Bodin, A. Ed. Department of Physical Geography, University of Stockholm, 37-39.
Karlén, W. and Denton, H. G., 1975: Holocene glacial variation in Sarek National Park, northern Sweden. *Boreas* **5**, 25-56.
Karlén, W., 1982: Holocene glacier fluctuations in Scandinavia. *Striae* **18**, 26-34.
Karlén, W., 1988: Scandivian glacial and climate fluctuations during the Holocene. *Quaternary Science Reviews* **7**, 199-209.
Karlén, W. and Kuylenstierna, J., 1996: On solar forcing of Holocene climate: evidence from Scandinavia. *The Holocene* **6**, 359-365.
Karlöf, L., Sidenbladh, A. and Schneider, T., 1996: Mass balance of Mårmaglaciären 1994/95. *Forskningsrapport* **103**. Jansson, P. Ed. Department of Physical Geography, University of Stockholm, 11-14.
Kattenberg, A., Giorgi, F., Grassl, H., Meehl, G. A., Mitchell, J. F. B., Stouffer, R. J., Tokioka, T., Weaver, A. J. and Wigley, T. M. L., 1996: *IPCC – Climate change 1995, the science of climate change*. Houghton, J. T., Meira Filho, L. G., Callander, B. A., Harris, N., Kattenberg, A., and Maskell, K. Eds.
Cambridge university press, Great Britain. 572 pp.
Kind, R. J., 1981: Snow drifting. *Handbook of snow*. Gray, D. M and Male, D. H. Eds. Pergamon Press, Ontario, Canada. 338-359. 776 pp.
Kullman, L., 1992: Orbital forcing and tree-limit history: hypothesis and preliminary interpretation of evidence from Swedish Lapland. *Holocene* **2**, 131-137.
Kuusisto, E., 1980: On the values and variability of degree-day melting factors in Finland. *Nord. Hydrol.* **11**, 235-242.
Lamb, H. H., 1995: *Climate history and the modern world*. 2nd edition, Routledge, London and New York. 433 pp.
Male, D. H. and Gray, D. M., 1981: *Handbook of snow*. Gray, D. M and Male, D. H. Eds. Pergamon Press, Ontario, Canada. 360-436. 776 pp.
Mörner, N. A. and Karlén, W., 1984: Climate changes on yearly to millennial bases: geological historical and instrumental records. Proceedings of the second Nordic Symposium on Climate Changes and Related Problems, Stockholm, Sweden, May 16-20, 1983. 667 pp.
Oerlemans, J., Räisänen, J. and Rummukainen, M., 1999: Forcing glacier models with climate scenarios calculated by SWECLIM. *Report from Department of Meteorology*, **DM-80** Stockholm University, October 1999, 8 pp.
Ohmura, A., Kasser, P. and Funk, M., 1992: Climate at the equilibrium line of glaciers. *Journal of Glaciology* **38**, 397-411.

Oke, T. R., 1987: *Boundary layer climate*. 2nd edition. Routledge, London. 435 pp.
Østrem, G., 1964: Ice-cored moraines in Scandinavia. *Geografiska Annaler* **46**, 282-337.
Pohjola, V. A. and Rogers, J. C., 1997: Coupling between the atmospheric circulation and extremes of the mass balance of Storglaciären, northern Scandinavia. *Annals of Glaciology* **24**, 229-233.
Räisänen, J., Rummukainen, M., Ullerstig, A., Bringfelt, B., Hansson, U. and Willén, U., 1999: The first Rossby Centre regional climate scenario – Dynamical downscaling of CO2-induced climate change in the HadCM2 GCM. *Reports Meteorology and Climatology*, **85**, SMHI, 56 pp.
Schaerer, P. A., 1981: Avalanches. *Handbook of snow*. Gray, D. M and Male, D. H. Eds. Pergamon Press, Ontario, Canada. 475-518. 776 pp.
Schneeberger, C., 1998: *Glacier Balance Modelling using a GCM*. Diploma Thesis at the Institute of Geography, Department of Geology, ETH, Zürich.
Skinner B. J. and Porter, S. P., 1987: *Physical Geology*. John Wiley & Sons, New York, USA. 750 pp.
Witmer, U., 1984: Eine Methode zur flächendeckenden Kartierung von Schneehöhen unter Berücksichtigung von reliefbedingten Einflüssen, *Geographica Bernensia* **G21**, Geographisch Institut der Universität, Bern, Switzerland.

Personal communication
Jansson, P., 1999. Department of Physical Geography, University of Stockholm.

Appendix A

Climate station description

The automatic weather station Aanderaa 2700 consists of:

- a hardware set for carrying the sensors, a sensor plug-in board, solar cell power unit, cables and connectors.
- sensors (Table A1).
- data storing unit model 2990, here the data from the data sampler is stored. Totally capacity 65530 10-bit words.

All instruments except ground temperature and relative humidity is placed two m above the ground. The relative humidity is placed in the locker with the hardware set and the data-storing unit. The climate station measures the weather data with three hours interval and this gives a momentary value each three hours. The sensors that measure the wind speed and the wind direction give an average value since the last readings (3 hours). The wind speed sensor also measures the max wind where the highest 2 seconds period in the last 3 hours are represented.

Table A1. Description of the sensors installed on the automatic weather station in the central cirque of the Rassepautasjtjåkka massif.

Sensor	Channel	Range	Accuracy	Description
Wind speed sensor 2740	2/3	60 m/s	± 2% or 20 m/s, whatever is the greater	Measures average and maximum wind speed during the sampling interval
Wind direction sensor 2750	4	0°=N 256°=E 512°=S 768°=W	Better than ± 5°	Measures wind direction
Solar radiation sensor (Pyranometer) 2770	5	0-200 mw/cm^2	± 3 mw/cm^2	Measures incoming short wavelength radiation in the range 0.3-2.5 microns.
Relative Humidity sensor 2820	6	5-100 RH	± 3%RH	Measures the relative humidity.
Air temperature sensor 2775	7	-44 to +49°C	0.1° (resolution)	Measures air temperature
Net atmospheric radiation sensor (Pyrradiometer) 2811	8	0-200mW/cm^2	3% of reading	Measures solar and thermal radiation in the wavelength range 0.3 to 60 microns
Air pressure sensor 2810	9	790 - 960 mb	± 0.2 mb	Measures air pressure
Temperature sensor 2812	10	-44 to +49°C	0.1° C (resolution)	Measures soil temperature.

Appendix B

Weather data collected from the Rassepautasjtjåkka massif

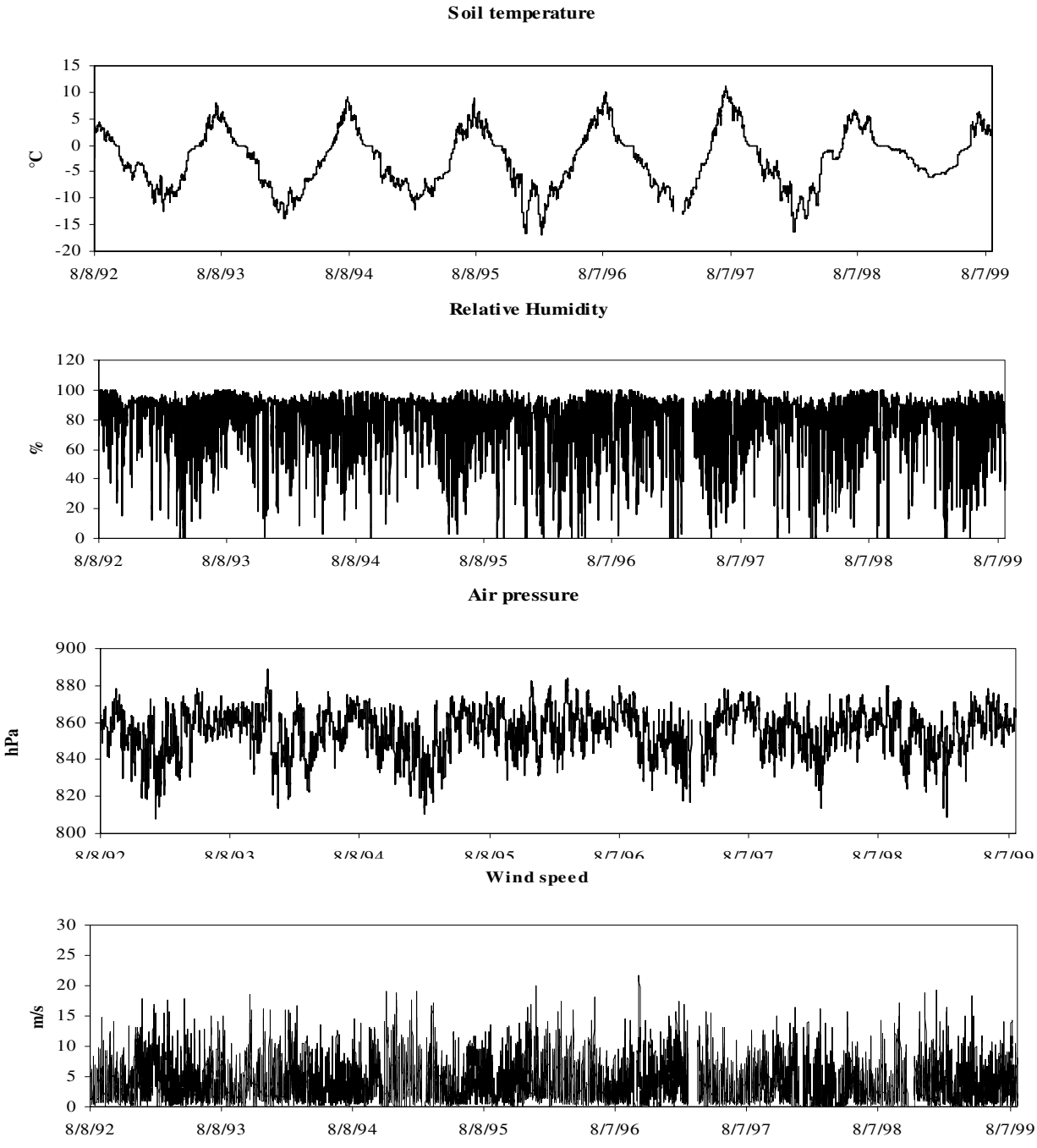

Figure A1. Weather data collected from the climate station, Rassepautasjtjåkka massif, 8 August 1992 to 27 August 1999. One-month break in the measurements occurred in February 1997.

Appendix C

Evaluation of the generalised snow depth

An evaluation of the assumption that the snow declines linearly between 10 and 60° was made to show how this would affect the measured point data. It should not exceed the already possible existing error (50 cm).

Table A2. A comparison between the measured and the generalised snow depth assuming that the snow declines linearly between 10 and 60°.

	X	Y	Measured snow depth (cm w. eq)	Generalised snow depth (cm w. eq.)	Difference (cm)
1993	1627500	7558000	33	30	9
	1627200	7558100	86	86	0
	1629500	7556000	70	70	0
	1629150	7556000	350	343	20
	1629150	7556100	350	350	0
	1629300	7556150	377	377	0
	1627350	7558100	56	56	0
	1627250	7558000	98	98	0
	1627150	7557950	119	119	0
	1627350	7557950	53	51	6
1995	1629887	7555862	21	21	0
	1629637	7556138	67	67	0
	1629286	7555913	88	64	**68**
	1629336	7555837	119	108	31
	1627300	7558000	63	63	0
	1627100	7558000	60	60	0
	1627050	7558050	77	77	0
	1627150	7558200	74	74	0
	1627250	7558400	14	12	6
	1629562	7556013	42	41	4
1999	1626822	7558477	47	46	4
	1626973	7558027	72	67	14
	1627373	7557817	60	58	6
	1626973	7558177	53	46	20
	1626762	7558027	28	24	11
	1629425	7555775	123	115	23
	1629665	7555985	11	11	0
	1629675	75566175	60	45	42
	1629214	7556025	84	83	4
	1629324	7556265	98	95	9

Lunds Universitets Naturgeografiska institution. Seminarieuppsatser. Uppsatserna finns tillgängliga på Naturgeografiska institutionens bibliotek, Sölvegatan 13, 223 62 LUND.

The reports are available at the Geo-Library, Department of Physical Geography, University of Lund, Sölvegatan 13, S-223 62 Lund, Sweden.

1. Pilesjö, P. (1985): Metoder för morfometrisk analys av kustområden.
2. Ahlström, K. & Bergman, A. (1986): Kartering av erosionskänsliga områden i Ringsjöbygden.
3. Huseid, A. (1986): Stormfällning och dess orsakssamband, Söderåsen, Skåne.
4. Sandstedt, P. & Wällstedt, B. (1986): Krankesjön under ytan - en naturgeografisk beskrivning.
5. Johansson, K. (1986): En lokalklimatisk temperaturstudie på Kungsmarken, öster om Lund.
6. Estgren, C. (1987): Isälvsstråket Djurfälla-Flädermo, norr om Motala.
7. Lindgren, E. & Runnström, M. (1987): En objektiv metod för att bestämma läplanteringars läverkan.
8. Hansson, R. (1987): Studie av frekvensstyrd filtringsmetod för att segmentera satellitbilder, med försök på Landsat TM-data över ett skogsområde i S. Norrland.
9. Matthiesen, N. & Snäll, M. (1988): Temperatur och himmelsexponering i gator: Resultat av mätningar i Malmö.

10A. Nilsson, S. (1988): Veberöd. En beskrivning av samhällets och bygdens utbyggnad och utveckling från början av 1800-talet till vår tid.

10B. Nilson, G., 1988: Isförhållande i södra Öresund.

11. Tunving, E. (1989): Översvämning i Murciaprovinsen, sydöstra Spanien, november 1987.
12. Glave, S. (1989): Termiska studier i Malmö med värmebilder och konventionell mätutrustning.
13. Mjölbo, Y. (1989): Landskapsförändringen - hur skall den övervakas?
14. Finnander, M-L. (1989): Vädrets betydelse för snöavsmältningen i Tarfaladalen.
15. Ardö, J. (1989): Samband mellan Landsat TM-data och skogliga beståndsdata på avdelningsnivå.
16. Mikaelsson, E. (1989): Byskeälvens dalgång inom Västerbottens län. Geomorfologisk karta, beskrivning och naturvärdesbedömning.
17. Nhilen, C. (1990): Bilavgaser i gatumiljö och deras beroende av vädret. Litteraturstudier och mätning med DOAS vid motortrafikled i Umeå.
18. Brasjö, C. (1990): Geometrisk korrektion av NOAA AVHRR-data.
19. Erlandsson, R. (1991): Vägbanetemperaturer i Lund.
20. Arheimer, B. (1991): Näringsläckage från åkermark inom Brååns dräneringsområde. Lokalisering och åtgärdsförslag.
21. Andersson, G. (1991): En studie av transversalmoräner i västra Småland.

22A. Skillius, Å., (1991): Water havesting in Bakul, Senegal.

22B. Persson, P. (1991): Satellitdata för övervakning av höstsådda rapsfält i Skåne.

23. Michelson, D. (1991): Land Use Mapping of theThat Luang - Salakham Wetland, Lao PDR, Using Landsat TM-Data.

24. Malmberg, U. (1991): En jämförelse mellan SPOT- och Landsatdata för vegetationsklassning i Småland.
25. Mossberg, M. & Pettersson, G. (1991): A Study of Infiltration Capacity in a Semiarid Environment, Mberengwa District, Zimbabwe.
26. Theander, T. (1992): Avfallsupplag i Malmöhus län. Dränering och miljöpåverkan.
27. Osaengius, S. (1992): Stranderosion vid Löderups strandbad.
28. Olsson, K. (1992): Sea Ice Dynamics in Time and Space. Based on upward looking sonar, satellite images and a time series of digital ice charts.
29. Larsson, K. (1993): Gully Erosion from Road Drainage in the Kenyan Highlands. A Study of Aerial Photo Interpreted Factors.
30. Richardson, C. (1993): Nischbildningsprocesser - en fältstudie vid Passglaciären, Kebnekaise.
31. Martinsson, L. (1994): Detection of Forest Change in Sumava Mountains, Czech Republic Using Remotely Sensed Data.
32. Klintenberg, P. (1995): The Vegetation Distribution in the Kärkevagge Valley.
33. Hese, S. (1995): Forest Damage Assessment in the Black Triangle area using Landsat TM, MSS and Forest Inventory data.
34. Josefsson, T. och Mårtensson, I. (1995). A vegetation map and a Digital Elevation Model over the Kapp Linné area, Svalbard -with analyses of the vertical and horizontal distribution of the vegetation
35. Brogaard, S och Falkenström, H. (1995). Assessing salinization, sand encroachment and expanding urban areas in the Nile Valley using Landsat MSS data.
36. Krantz, M. (1996): GIS som hjälpmedel vid växtskyddsrådgivning.
37. Lindegård, P. (1996). VINTERKLIMAT OCH VÅRBAKSLAG. Lufttemperatur och kådflödessjuka hos gran i södra Sverige.
38. Bremborg, P. (1996). Desertification mapping of Horqin Sandy Land, Inner Mongolia, by means of remote sensing.
39. Hellberg, J. (1996). Förändringsstudie av jordbrukslandskapet på Söderslätt 1938-1985.
40. Achberger, C. (1996): Quality and representability of mobile measurements for local climatological research.
41. Olsson, M. (1996): Extrema lufttryck i Europa och Skandinavien 1881-1995
42. Sundberg, D. (1997): En GIS-tillämpad studie av vattenerosion i sydsvensk jordbruksmark.
43. Liljeberg, M. (1997): Klassning och statistisk separabilitetsanalys av marktäckningsklasser i Halland, analys av multivariata data Landsat TM och ERS-1 SAR.
44. Roos, E. (1997): Temperature Variations and Landscape Heterogeneity in two Swedish Agricultural Areas. An application of mobile measurements.
45. Arvidsson, P. (1997): Regional fördelning av skogsskador i förhållande till mängd SO_2 under vegetationsperioden i norra Tjeckien.
46. Akselsson, C. (1997): Kritisk belastning av aciditet för skogsmark i norra Tjeckien.
47. Carlsson, G. (1997): Turbulens och supraglacial meandring.
48. Jönsson, C. (1998): Multitemporala vegetationsstudier i nordöstra Kenya med

AVHRR NDVI

49. Kolmert, S. (1998): Evaluation of a conceptual semi-distributed hydrological model – A case study of Hörbyån.
50. Persson, A. (1998): Kartering av markanvändning med meteorologisk satellitdata för förbättring av en atmosfärisk spridningsmodell.
51. Andersson, U. och Nilsson, D. (1998): Distributed hydrological modelling in a GIS perspective – an evaluation of the MIKE SHE model.
52. Andersson, K. och Carlstedt, J. (1998): Different GIS and remote sensing techniques for detection of changes in vegetation cover - A study in the Nam Ngum and Nam Lik catchment areas in the Lao PDR.
53. Andersson, J., (1999): Användning av global satllitdata för uppskattning av spannmålsproduktion i västafrikanska Sahel.
54. Flodmark, A.E., (1999): Urban Geographic Information Systems, The City of Berkeley Pilot GIS

55A. Lyborg, Jessic & Thurfell, Lilian (1999): Forest damage, water flow and digital elevation models: a case study of the Krkonose National Park, Czech Republic.

55B. Tagesson, I., och Wramneby, A., (1999): Kväveläckage inom Tolångaåns dräneringsområde – modellering och åtgärdssimulering.

56. Almkvist, E., (1999): Högfrekventa tryckvariationer under de senaste århundradena.
57. Alstorp, P., och Johansson, T., (1999): Översiktlig buller- och luftföroreningsinventering i Burlövs Kommun år 1994 med hjälp av geografiska i informationssystem – möjligheter och begränsningar.
58. Mattsson, F., (1999): Analys av molnklotter med IRST-data inom det termala infraröda våglängdsområdet
59. Hallgren, L., och Johansson, A., (1999): Analysing land cover changes in the Caprivi Strip, Namibia, using Landsat TM and Spot XS imagery.
60. Granhäll, T., (1999): Aerosolers dygnsvariationer och långväga transporter.
61. Kjellander, C., (1999): Variations in the energy budget above growing wheat and barley, Ilstorp 1998 - a gradient-profile approach
62. Moskvitina, M., (1999): GIS as a Tool for Environmental Impact Assessment - A case study of EIA implementation for the road building project in Strömstad, Sweden
63. Eriksson, H., (1999): Undersökning av sambandet mellan strålningstemperatur och NDVI i Sahel.
64. Elmqvist, B., Lundström, J., (2000): The utility of NOAA AVHRR data for vegetation studies in semi-arid regions.
65. Wickberg, J., (2000): GIS och statistik vid dräneringsområdesvis kväveläckagebeskrivning i Halland
66. Johansson, M., (2000): Climate conditions required for re-glaciation of cirques in Rassepautasjtjåkka massif, northern Sweden.